INTERNATIONAL JOURNAL OF
NUMERICAL ANALYSIS AND MODELING
Volume 21, Number 2, Pages 244–267

doi: 10.4208/ijnam2024-1010

TWO DECOUPLED AND LINEARIZED BLOCK-CENTERED FINITE DIFFERENCE METHODS FOR THE NONLINEAR SYMMETRIC REGULARIZED LONG WAVE EQUATION

JIE XU, SHUSEN XIE, AND HONGFEI FU*

Abstract. In this paper, by introducing a new flux variable, two decoupled and linearized block-centered finite difference methods are developed and analyzed for the nonlinear symmetric regularized long wave equation, where the two-step backward difference formula and Crank-Nicolson temporal discretization combined with linear extrapolation technique are employed. Under a reasonable time stepsize ratio restriction, i.e., $\Delta t = o(h^{1/4})$, second-order convergence for both the primal variable and its flux are rigorously proved on general non-uniform spatial grids. Moreover, based upon the convergence results and inverse estimate, stability of two methods are also demonstrated. Ample numerical experiments are presented to confirm the theoretical analysis.

Key words. Symmetric regularized long wave equation, backward difference formula, Crank-Nicolson, block-centered finite difference method, error estimates.

1. Introduction

Decades ago, numerical simulations of the mathematical models to explain the behavior of nonlinear wave phenomena began to become one of the important scientific research fields. Many nonlinear wave systems are usually used to demonstrate some typical physical problems, such as heat flow phenomena, wave and shallow water wave propagation, optical fiber, hydrodynamics, plasma physics, chemical kinematics, electricity, biology and quantum mechanics [2, 3, 7, 20, 29].

As one of the wave models, the symmetric regularized long wave (SRLW) equation can describe various nonlinear phenomena. The first research result devoted to this model was published by Seyler and Fenstermacher [27] for describing the propagation of ion acoustic waves, shallow water waves, and solitary waves with bidirectional propagation:

$$u_t - u_{xxt} + \rho_x + uu_x = 0, \tag{1}$$

$$\rho_t + u_x = 0, \tag{2}$$

for $(x,t) \in Q = I \times J := (a,b) \times (0,T]$, where ρ and u are dimensionless electron charge density and the fluid velocity, respectively.

In this paper, we are interested to propose two decoupled and linearized finite difference methods on general *non-uniform* spatial grids for (1)–(2) enclosed with the following boundary and initial conditions

$$u_x(a,t) = u_x(b,t) = \rho(a,t) = \rho(b,t) = 0, \quad t \in J, \tag{3}$$

$$u(x,0) = u^o(x), \quad \rho(x,0) = \rho^o(x), \quad x \in \bar{I}, \tag{4}$$

where $u_0(x)$ and $\rho_0(x)$ are two given smooth functions.

Up to now, there are a great amount of work devoting to the traveling wave solution and numerical simulations of the SRLW equation. Existence and uniqueness

Received by the editors on October 11, 2022 and, accepted on January 16, 2024.
2000 *Mathematics Subject Classification.* 65H10, 65M06, 65M12.
*Corresponding author.

of the solution, existence of global attractors, stability and instability of solitary waves and exact traveling wave solution were studied in Refs. [5, 6, 9, 32]. However, the analytical solution of model (1)–(2) is usually not available on bounded domain. Therefore, efficient numerical methods and numerical analysis are necessary, of which the finite difference method is viewed as one of the most significant numerical methods. In Ref. [31], Wang, Zhang and Chen proposed three nonlinear and linear three-level second-order difference schemes on *uniform* spatial grids, in which two are coupled and one is decoupled. The convergence estimates of the approximate solutions to u and ρ were proved to be $\mathcal{O}(\Delta t^2 + h^2)$ in discrete L^∞ and L^2 norm, respectively. Li [19] studied a conservative weighted compact difference method on *uniform* grids as well, and proved that the convergence order is $\mathcal{O}(\Delta t^2 + h^4)$ in discrete L^∞ norm for u and L^2 norm for ρ, respectively. Recently, He et al. [13] constructed a fourth-order accurate compact difference scheme for the SRLW equation, and they also analyzed the convergence and stability of the scheme, but only for u in discrete L^∞ norm with a *uniform* spatial grids. Besides, In Ref. [14], He, Wang and Dai developed two dissipative difference schemes for the generalized SRLW equations, where one is a two-level nonlinear coupled scheme and the other is a three-level linear decoupled scheme. Convergence order $\mathcal{O}(\Delta t^2 + h^4)$ on *uniform* spatial grids and stability in discrete L^∞ norm for u and L^2 norm for ρ were proved by the discrete energy method. Dirichlet boundary conditions are involved in all papers mentioned above. There are also some other numerical methods for the SRLW model, see finite difference methods [4, 12, 16, 21, 24, 36], spectral and pseudo spectral methods [10, 18, 28, 37, 38], and finite element methods [11, 22, 23, 34]. However, as far as we know, there are still no papers concerning finite difference methods on general *non-uniform* meshes.

In real simulations of the nonlinear SRLW equation, the flux of the primal variable usually represents the velocity variation, and sometimes it is of great importance to calculate the flux in high-order accuracy, which is also the motivation of our concern on space discritization. It is well known that block-centered finite difference (BCFD) method can simultaneously approximate the primal variable and its flux to a same order of accuracy on non-uniform grids without any accuracy lost, compared to the standard finite difference method. It can be thought of as the lowest-order Raviart-Thomas mixed element method [26] by employing a proper numerical quadrature formula. Thus, the method is widely studied in the literature. For example, Weiser and Wheeler [30] studied the BCFD method for elliptic problems with Neumann boundary conditions in one and two-dimensional cases. They demonstrated that with sufficiently smooth data, the discrete L^2-norm errors for both the approximate solution and its first derivatives are in second-order for all non-uniform grids. In Ref. [1], Arbogast, Wheeler and Yotov presented the mixed finite elements for elliptic problems with tensor coefficients as cell-centered finite differences. Besides, in Refs. [17, 25, 35], some BCFD methods were developed to solve flow models such as the multiscale flows model, Darcy-Forchheimer model, and semiconductor device model. Basically, second-order spatial convergence were observed therein. In summary, the BCFD method could keep second-order spatial accuracy both for the original unknown, called pressure in porous media flow, and its derivatives, called velocity in porous media flow, on general non-uniform spatial grids. Thus, it is widely used even for problems with boundary layers and large gradient deformations.

As far as we know, there seems to be no published work on BCFD method for the nonlinear SRLW equation with Neumann boundary conditions. Our main goal

is to present linearized two-step backward difference formula (BDF2) and Crank-Nicolson (CN) time discretization BCFD methods (denoted as BDF2-BCFD and CN-BCFD) for this model, and by using a mathematical induction argument to prove second-order time and space accuracy on *non-uniform* spatial grids with respect to discrete norms. The proposed schemes have a series of advantages:

- The solution procedures are linearly implicit with tri-diagonal system and decoupled, which are much more efficient than a coupled fully nonlinear implicit method.
- Second-order convergence in time and space are rigorously proved on *non-uniform* spatial grids, while other finite difference methods are usually constructed and analyzed on *uniform* spatial grids.
- The primal variable and its flux can be calculated simultaneously, and they maintain the same order of accuracy, while direct difference methods usually cause a reduction of convergence order for the flux.

The rest of the paper is organized as follows. In section 2, notations and preliminaries are given, and the linearized BDF2-BCFD scheme and CN-BCFD scheme are proposed. In section 3, convergence of both schemes are rigorously proved via the discrete energy method and the mathematical induction argument. Based upon the convergence results, stability conclusions for the schemes are carried out in section 4. Numerical experiments are given in section 5, in which the accuracy and efficiency of both linearized methods are verified. Finally, we draw some conclusions and discuss future work in the last section. Throughout this paper, we use C to denote a generic positive constant which is independent of grid parameters and may take different values at different places.

2. Two decoupled and linearized second-order BCFD schemes

Let $p = -u_x$, then (1)–(4) can be written as

$$u_t + p_{xt} + \rho_x - up = 0, \tag{5}$$

$$\rho_t - p = 0, \tag{6}$$

$$p + u_x = 0, \tag{7}$$

for $(x,t) \in Q$, enclosed with boundary and initial conditions

$$p(a,t) = p(b,t) = \rho(a,t) = \rho(b,t) = 0, \quad t \in J, \tag{8}$$

$$u(x,0) = u^o(x), \quad \rho(x,0) = \rho^o(x), \quad x \in \bar{I}. \tag{9}$$

In this paper, we shall start from (5)–(9) to develop two decoupled and linearized BCFD schemes, where the primal variables u, ρ and flux p are approximated simultaneously, and the same second-order spatial accuracy are achieved for them on general non-uniform staggered spatial grids.

Below we first introduce some basic notations and preliminary results that needed in the following sections.

2.1. Notations and preliminaries. Let N be a positive integer and $t^n = n\Delta t$ $(0 \le n \le N)$ with $\Delta t := T/N$ be a given sequence. For temporal grid function $\{\phi^n\}_{n=0}^N$, define

$$\delta_t \phi^n = \frac{\phi^n - \phi^{n-1}}{\Delta t}, \ D_t \phi^n := \frac{3\phi^n - 4\phi^{n-1} + \phi^{n-2}}{2\Delta t},$$

$$\hat{D}_t \phi^n := \frac{3\phi^n - 4\phi^{n+1} + \phi^{n+2}}{2\Delta t}, \ \hat{\phi}^{n-1/2} := \frac{\phi^n + \phi^{n-1}}{2},$$

$$\phi^{n,*}=\begin{cases}\phi^0, & n=1,\\ 2\phi^{n-1}-\phi^{n-2}, & n\geq 2,\end{cases}\quad \phi^{n,\star}=\begin{cases}\phi^0, & n=1,\\ \frac{3}{2}\phi^{n-1}-\frac{1}{2}\phi^{n-2}, & n\geq 2.\end{cases}$$

Let M be another positive integer, and define a set of spatial partition of $[a,b]$ as

$$\Pi_h:\ a=x_{1/2}<x_{3/2}<\cdots<x_{M-1/2}<x_{M+1/2}=b,$$

with grid sizes $h_i:=x_{i+1/2}-x_{i-1/2}$ for $i=1,2,\ldots,M$. Let $h:=\max_{1\leq i\leq M}h_i$. We assume that the grid partition Π_h is regular, i.e., there exists a positive constant σ such that $h\leq\sigma\min_{1\leq i\leq M}h_i$. As seen in the next section, the unknowns ρ and p are approximated on Π_h. Besides, the unknown u shall be approximated on another set of spatial grids

$$\Pi_h^*:x_i:=\frac{x_{i+1/2}+x_{i-1/2}}{2},\ i=1,2,\ldots,M,$$

with grid sizes $h_{1/2}:=x_1-a$, $h_{i+1/2}:=x_{i+1}-x_i$ for $1\leq i\leq M$, and $h_{M+1/2}:=b-x_M$. It is easy to check that

$$h_{1/2}=\frac{h_1}{2};\ h_{i+1/2}=\frac{h_{i+1}+h_i}{2},\ 1\leq i\leq M;\ h_{M+1/2}=\frac{h_M}{2},$$

and therefore the partition Π_h^* is also regular. Furthermore, for spatial grid functions $\{\phi_i\}_{i=1}^M$ and $\{\psi_{i+1/2}\}_{i=0}^M$, define

$$d_h\phi_{i+1/2}:=\frac{\phi_{i+1}-\phi_i}{h_{i+1/2}},\quad D_h\psi_i:=\frac{\psi_{i+1/2}-\psi_{i-1/2}}{h_i},\quad \bar{\psi}_i:=\frac{\psi_{i+1/2}+\psi_{i-1/2}}{2}.$$

In addition, we introduce the discrete inner products and norms on Π_h^* and Π_h, respectively

$$\begin{aligned}(f,g)_{\mathrm{M}}&:=\sum_{i=1}^{M}h_if_ig_i,\quad \|f\|_{\mathrm{M}}^2=(f,f)_{\mathrm{M}},\\ (f,g)_{\mathrm{T}}&:=\sum_{i=1}^{M-1}h_{i+1/2}f_{i+1/2}g_{i+1/2},\quad \|f\|_{\mathrm{T}}^2=(f,f)_{\mathrm{T}}.\end{aligned}\tag{10}$$

Lemma 2.1 ([30]). *Let $\{q_i\}_{i=1}^M$ and $\{w_{i+1/2}\}_{i=0}^M$ be any grid functions such that $w_{1/2}=w_{M+1/2}=0$, then there holds*

$$(D_hw,q)_{\mathrm{M}}=-(w,d_hq)_{\mathrm{T}}.$$

Lemma 2.2 ([33]). *For any arbitrary grid function $\{\psi_{i+1/2}\}_{i=0}^M$ with $\psi_{1/2}=\psi_{M+1/2}=0$, it holds*

$$\|\bar{\psi}\|_{\mathrm{M}}\leq\|\psi\|_{\mathrm{T}}.$$

2.2. Two decoupled and linearized BCFD schemes. At each time level t^n, let $G^n:=\{G_{i+1/2}^n\}$, $P^n:=\{P_{i+1/2}^n\}$ and $U^n:=\{U_i^n\}$ be respectively the finite difference approximations of $\rho^n:=\{\rho(x_{i+1/2},t^n)\}$, $p^n:=\{p(x_{i+1/2},t^n)\}$ and $u^n:=\{u(x_i,t^n)\}$.

In this subsection, a linearized two-step BDF type BCFD algorithm, named BDF2-BCFD, is first come up to solve the nonlinear SRLW equation (5)–(7), in which the BDF2 method and linear extrapolation technique are used in time discretization and block-centered finite difference method is considered in space discretization on general non-uniform staggered spatial grids. To fix the idea, the

linearized BDF2-BCFD method for the approximation of (5)–(7) is proposed as follows:

$$D_t U_i^n + D_t[D_h P_i^n] + D_h G_i^n - U_i^{n,*}\ \bar{P}_i^n = 0, \quad i = 1, \ldots, M, \tag{11}$$

$$D_t G_{i+1/2}^n - P_{i+1/2}^n = 0, \quad i = 1, \ldots, M-1; \quad G_{1/2}^n = G_{M+1/2}^n = 0, \tag{12}$$

$$P_{i+1/2}^n + d_h U_{i+1/2}^n = 0, \quad i = 1, \ldots, M-1; \quad P_{1/2}^n = P_{M+1/2}^n = 0, \tag{13}$$

for $n \geq 2$. In particular, for $n = 1$, i.e., the first time level, we use the following scheme to compute $\{U^1, P^1, G^1\}$:

$$\delta_t U_i^1 + \delta_t[D_h P_i^1] + D_h \hat{G}_i^{1/2} - U_i^0\ \hat{\bar{P}}_i^{1/2} = 0, \quad i = 1, \ldots, M, \tag{14}$$

$$\delta_t G_{i+1/2}^1 - \hat{P}_{i+1/2}^{1/2} = 0, \quad i = 1, \ldots, M-1; \quad G_{1/2}^1 = G_{M+1/2}^1 = 0, \tag{15}$$

$$P_{i+1/2}^1 + d_h U_{i+1/2}^1 = 0, \quad i = 1, \ldots, M-1; \quad P_{1/2}^1 = P_{M+1/2}^1 = 0, \tag{16}$$

which is enclosed with the following initial conditions

$$U_i^0 = u^o(x_i),\ P_{i+1/2}^0 = -u_x^o\left(x_{i+1/2}\right),\ G_{i+1/2}^0 = \rho^o(x_{i+1/2}). \tag{17}$$

Remark 2.1. In this scheme, we use a second-order extrapolation at time level t^n to approximate the solution u in the nonlinear term up, which leads to a linear scheme for the nonliear SRLW equation. From the computational viewpoint, we insert equations (12)–(13) into (11) to derive a decoupled system which only involves the approximate solution U^n $(n \geq 2)$:

$$\begin{aligned} &D_t U_i^n - D_t[d_h(D_h U_i^n)] - \frac{2}{3} d_h(D_h U_i^n) + U_i^{n,*}\ d_h \bar{U}_i^n \\ &\quad = -\frac{4}{3} D_h G_i^{n-1} + \frac{1}{3} D_h G_i^{n-2}, \end{aligned} \tag{18}$$

for $i = 1, \ldots, M$.

We remark that at each time level t^n, system (18) is linear and tri-diagonal, and thus can be solved via the classical Thomas algorithm in only $\mathcal{O}(M)$ operation, which is much more computationally efficient than to solve a coupled system. Once U^n is obtained, P^n is computed explicitly by using (13), and finally, G^n is also obtained explicitly via (12). For the case $n = 1$, the same procedures can be applied to the step (14)–(16).

Next, if the Crank-Nicolson method and linear extrapolation technique are employed in time discretization, a linearized Crank-Nicolson type BCFD method, named CN-BCFD, can also be proposed to solve the nonlinear SRLW equation (5)–(7):

$$\delta_t U_i^n + \delta_t[D_h P_i^n] + D_h \hat{G}_i^{n-1/2} - U_i^{n,\star} \hat{\bar{P}}_i^{n-1/2} = 0, \quad i = 1, \ldots, M, \tag{19}$$

$$\delta_t G_{i+1/2}^n - \hat{P}_{i+1/2}^{n-1/2} = 0, \quad i = 1, \ldots, M-1; \quad G_{1/2}^n = G_{M+1/2}^n = 0 \tag{20}$$

$$P_{i+1/2}^n + d_h U_{i+1/2}^n = 0, \quad i = 1, \ldots, M-1; \quad P_{1/2}^n = P_{M+1/2}^n = 0, \tag{21}$$

for $n \geq 1$, in which initial conditions are given by (17).

Remark 2.2. The main difference from the linearized BDF2-BCFD scheme is that the Crank-Nicolson time discretization method is adopted there. Therefore, a second-order extrapolation at the time level $t^{n-1/2}$ has to be adopted to approximate the solution u in the nonlinear term up. The computational procedure is basically the same as that in Remark 2.1, and the solutions U^n, P^n and G^n are also decoupled.

3. Error estimates for the linearized BCFD schemes

In this section, we shall show the convergence estimates of the two developed linearized BCFD algorithms. Throughout the paper, we make the following smoothness assumptions:

$$u(x,t),\ p(x,t),\ \rho(x,t) \in C^3(\bar{Q}). \tag{22}$$

and suppose there exists a positive constant L such that

$$\max_{(x,t)\in\bar{Q}} \{|u(x,t)|, |p(x,t)|\} \le L. \tag{23}$$

As the non-uniform spatial mesh is employed, we can see that the truncation errors of the difference operator d_h in (13) and (21) are only first-order accurate in space. However, following the idea of Rui et al. [25], we can introduce a second-order correction term

$$\eta_i^n := -\frac{h_i^2}{8}[u_{xx}]_i^n = \mathcal{O}(h^2), \quad i = 1, \dots, M, \tag{24}$$

to ensure the global second-order spatial convergence of the linearized BCFD schemes (11)–(13) and (19)–(21).

For $n = 2, \dots, N$, set

$$\omega_i^n := D_t\eta_i^n, \quad \tilde{\omega}_i^n := \delta_t\eta_i^n, \quad i = 1, \dots, M. \tag{25}$$

It is clear that for $u \in C^1\left([0,T]; C^2[a,b]\right)$,

$$\begin{aligned} |\omega_i^n| = |D_t\eta_i^n| &\le \frac{3}{\Delta t}\int_{t^{n-1}}^{t^n} \left|\frac{\partial \eta_i}{\partial t}\right| dt + \frac{1}{\Delta t}\int_{t^{n-2}}^{t^{n-1}} \left|\frac{\partial \eta_i}{\partial t}\right| dt \\ &\le Ch^2 \left\|u_{xxt}\right\|_{L^\infty(\bar{Q})} = \mathcal{O}(h^2), \quad i = 1, \dots, M. \end{aligned} \tag{26}$$

Similarly, we can prove

$$|\tilde{\omega}_i^n| = \mathcal{O}(h^2), \quad i = 1, \dots, M. \tag{27}$$

Lemma 3.1 ([25]). *Assume that condition (22) holds, then we have for $i = 1, \dots, M-1$,*

$$[u_x]_{i+1/2}^n = d_h(u+\eta)_{i+1/2}^n - \xi_{i+1/2}^n, \tag{28}$$

and the following approximate properties hold

$$\xi_{i+1/2}^n = \mathcal{O}(h^2),\ \left|\delta_t\xi_{i+1/2}^n\right| = \mathcal{O}(h^2),\ \left|\hat{D}_t\xi_{i+1/2}^n\right| = \mathcal{O}(h^2), \quad n = 1, \dots, N.$$

Let $\theta^n := u^n - U^n$, $\mu^n := p^n - P^n$, $\lambda^n := \rho^n - G^n$, for $n = 1, \dots, N$. Due to the second-order extrapolation used in the linearized BCFD methods, we pay special attention to error estimates for the scheme (14)–(16) (also (19)–(21) with $n = 1$) at first time level.

Theorem 3.1. *Assume that (22) holds, then we have*

$$\left\|u^1 - U^1\right\|_{\mathrm{M}} + \left\|p^1 - P^1\right\|_{\mathrm{T}} + \left\|\rho^1 - G^1\right\|_{\mathrm{T}} \le C\left(\Delta t^2 + h^2\right),$$

where C is a positive constant independent of Δt and h.

Proof. We see from (5)–(7) that the exact solutions $u_i^1 = u(x_i, t^1)$, $p_{i+1/2}^1 = p(x_{i+1/2}, t^1)$ and $\rho_{i+1/2}^1 = \rho(x_{i+1/2}, t^1)$ satisfy

$$\delta_t u_i^1 + \delta_t[D_h p_i^1] + D_h\hat{\rho}_i^{1/2} - u_i^0\,\hat{\hat{p}}_i^{1/2} = S_{1,i}^1 - S_{2,i}^1, \quad i = 1, \dots, M, \tag{29}$$

$$\delta_t\rho_{i+1/2}^1 - \hat{p}_{i+1/2}^{1/2} = S_{3,i+1/2}^1, \quad i = 1, \dots, M-1, \tag{30}$$

$$p^1_{i+1/2} + d_h(u+\eta)^1_{i+1/2} = \xi^1_{i+1/2}, \quad i = 1, \ldots, M-1, \tag{31}$$

$$\rho^1_{1/2} = \rho^1_{M+1/2} = 0, \quad p^1_{1/2} = p^1_{M+1/2} = 0, \tag{32}$$

with truncation errors

$$\begin{aligned} S^1_{1,i} &:= \left(\delta_t u^1_i - [u_t]^{1/2}_i\right) + \left(\delta_t[D_h p^1_i] - [p_{xt}]^{1/2}_i\right) + \left(D_h\hat{\rho}^{1/2}_i - [\rho_x]^{1/2}_i\right), \\ S^1_{2,i} &:= u^0_i \hat{\bar{p}}^{1/2}_i - [up]^{1/2}_i, \\ S^1_{3,i+1/2} &:= \left(\delta_t \rho^1_{i+1/2} - [\rho_t]^{1/2}_{i+1/2}\right) - \left(\hat{p}^{1/2}_{i+1/2} - p^{1/2}_{i+1/2}\right), \end{aligned}$$

and η^1, ξ^1 are defined respectively by (24) and (28). Moreover, by using the Taylor expansion, the above truncation errors can be directly estimated as

$$\begin{aligned} |S^1_{1,i}| &\le C\Delta t^2 \left(\|u_{ttt}\|_{L^\infty(\bar{Q})} + \|p_{xttt}\|_{L^\infty(\bar{Q})} + \|\rho_{xtt}\|_{L^\infty(\bar{Q})}\right) \\ &\quad + Ch^2 \left(\|p_{xxxt}\|_{L^\infty(\bar{Q})} + \|\rho_{xxx}\|_{L^\infty(\bar{Q})}\right) = \mathcal{O}(\Delta t^2 + h^2), \\ |S^1_{2,i}| &\le C\left(\Delta t^2 \|up_{tt}\|_{L^\infty(\bar{Q})} + h^2 \|up_{xx}\|_{L^\infty(\bar{Q})} + \Delta t \|u_t p\|_{L^\infty(\bar{Q})}\right) = \mathcal{O}(\Delta t + h^2), \\ |S^1_{3,i-1/2}| &\le C\Delta t^2 \left(\|\rho_{ttt}\|_{L^\infty(\bar{Q})} + \|p_{tt}\|_{L^\infty(\bar{Q})}\right) = \mathcal{O}(\Delta t^2), \end{aligned}$$

from which and the definition of the discrete norms in (10), we obtain

$$\|S^1_1\|_{\mathrm{M}} = \mathcal{O}(\Delta t^2 + h^2), \quad \|S^1_2\|_{\mathrm{M}} = \mathcal{O}(\Delta t + h^2), \quad \|S^1_3\|_{\mathrm{T}} = \mathcal{O}(\Delta t^2). \tag{33}$$

Noticing that $\theta^0 = \mu^0 = \lambda^0 = 0$, we conclude from (29)–(31) and (14)–(16) that the error equations at $t = t^1$ can be expressed as

$$\begin{aligned} &(\theta+\eta)^1_i + D_h\mu^1_i + \frac{\Delta t}{2} D_h\lambda^1_i - \frac{\Delta t}{2} u^0_i \bar{\mu}^1_i \\ &\qquad = \Delta t\left(S^1_{1,i} - S^1_{2,i}\right) + \eta^1_i, \quad i = 1, \ldots, M, \end{aligned} \tag{34}$$

$$\lambda^1_{i+1/2} - \frac{\Delta t}{2}\mu^1_{i+1/2} = \Delta t\, S^1_{3,i+1/2}, \quad i = 1, \ldots, M-1, \tag{35}$$

$$\mu^1_{i+1/2} + d_h(\theta+\eta)^1_{i+1/2} = \xi^1_{i+1/2}, \quad i = 1, \ldots, M-1, \tag{36}$$

$$\lambda^1_{1/2} = \lambda^1_{M+1/2} = 0, \quad \mu^1_{1/2} = \mu^1_{M+1/2}. \tag{37}$$

Now, taking discrete inner products with $\theta^1 + \eta^1$, λ^1 and μ^1, respectively, for (34), (35) and (36), we derive

$$\begin{aligned} &\left(\theta^1+\eta^1, \theta^1+\eta^1\right)_{\mathrm{M}} + \left(D_h\mu^1, \theta^1+\eta^1\right)_{\mathrm{M}} + \frac{\Delta t}{2}\left(D_h\lambda^1, \theta^1+\eta^1\right)_{\mathrm{M}} \\ &\quad - \frac{\Delta t}{2}\left(u^0\bar{\mu}^1, \theta^1+\eta^1\right)_{\mathrm{M}} = \Delta t\left(S^1_1 - S^1_2, \theta^1+\eta^1\right)_{\mathrm{M}} + \left(\eta^1, \theta^1+\eta^1\right)_{\mathrm{M}}, \end{aligned} \tag{38}$$

$$\left(\lambda^1, \lambda^1\right)_{\mathrm{T}} - \frac{\Delta t}{2}\left(\mu^1, \lambda^1\right)_{\mathrm{T}} = \Delta t\left(S^1_3, \lambda^1\right)_{\mathrm{T}}, \tag{39}$$

$$\left(\mu^1, \mu^1\right)_{\mathrm{T}} + \left(d_h(\theta+\eta)^1, \mu^1\right)_{\mathrm{T}} = \left(\xi^1, \mu^1\right)_{\mathrm{T}}. \tag{40}$$

Note that Lemma 2.1 and (36) imply that

$$\left(D_h\mu^1, \theta^1+\eta^1\right)_{\mathrm{M}} = -\left(d_h(\theta+\eta)^1, \mu^1\right)_{\mathrm{T}}, \tag{41}$$

$$\left(D_h\lambda^1, \theta^1+\eta^1\right)_{\mathrm{M}} = -\left(d_h(\theta+\eta)^1, \lambda^1\right)_{\mathrm{T}} = \left(\mu^1, \lambda^1\right)_{\mathrm{T}} - \left(\xi^1, \lambda^1\right)_{\mathrm{T}}. \tag{42}$$

Therefore, adding (38)–(40) together, and utilizing (41)–(42), by Young's inequality and Lemma 2.2, we have

$$\begin{aligned}
&\left\|\theta^1+\eta^1\right\|_{\mathrm{M}}^2+\left\|\mu^1\right\|_{\mathrm{T}}^2+\left\|\lambda^1\right\|_{\mathrm{T}}^2\\
&=\Delta t\left(S_1^1-S_2^1,\theta^1+\eta^1\right)_{\mathrm{M}}+\Delta t\left(S_3^1,\lambda^1\right)_{\mathrm{T}}+\frac{\Delta t}{2}\left(\xi^1,\lambda^1\right)_{\mathrm{T}}+\left(\eta^1,\theta^1+\eta^1\right)_{\mathrm{M}}\\
&\quad+\left(\xi^1,\mu^1\right)_{\mathrm{T}}+\frac{\Delta t}{2}\left(u^0\bar{\mu}^1,\theta^1+\eta^1\right)_{\mathrm{M}}\\
&\leq C_\epsilon\Delta t^2\left(\left\|S_1^1\right\|_{\mathrm{M}}^2+\left\|S_2^1\right\|_{\mathrm{M}}^2+\left\|S_3^1\right\|_{\mathrm{T}}^2+\left\|\xi^1\right\|_{\mathrm{T}}^2\right)+C_\epsilon\left(\left\|\eta^1\right\|_{\mathrm{M}}^2+\left\|\xi^1\right\|_{\mathrm{T}}^2\right)\\
&\quad+\epsilon\left(\left\|\theta^1+\eta^1\right\|_{\mathrm{M}}^2+\left\|\mu^1\right\|_{\mathrm{T}}^2+\left\|\lambda^1\right\|_{\mathrm{T}}^2\right)+\frac{\Delta tL}{4}\left(\left\|\theta^1+\eta^1\right\|_{\mathrm{M}}^2+\left\|\mu^1\right\|_{\mathrm{T}}^2\right),
\end{aligned}$$

where ϵ is a sufficiently small positive constant, and L is defined by (23).

If Δt and ϵ are chosen small enough, see $\Delta t\leq\frac{2(1-2\epsilon)}{L}$ and $\epsilon<1/2$, we conclude from (33), (24), and the estimate in Lemma 3.1 that

$$\left\|\theta^1+\eta^1\right\|_{\mathrm{M}}^2+\left\|\mu^1\right\|_{\mathrm{T}}^2+\left\|\lambda^1\right\|_{\mathrm{T}}^2\leq C\left(\Delta t^4+h^4\right), \tag{43}$$

which implies via the triangle inequality,

$$\left\|u^1-U^1\right\|_{\mathrm{M}}+\left\|p^1-P^1\right\|_{\mathrm{T}}+\left\|\rho^1-G^1\right\|_{\mathrm{T}}\leq C\left(\Delta t^2+h^2\right).$$

Therefore, the proof of Theorem 3.1 is completed. □

3.1. Error estimate of the linearized BDF2-BCFD scheme. Next, we consider the convergence of the linearized BDF2-BCFD scheme (11)–(13) for $n\geq 2$. We have the following main conclusion.

Theorem 3.2. *Assume that (22) holds. Under a time stepsize ratio restriction $\Delta t=o(h^{1/4})$, we have*

$$\left\|U^n\right\|_\infty\leq L+1, \tag{44}$$

and

$$\left\|u^n-U^n\right\|_{\mathrm{M}}+\left\|p^n-P^n\right\|_{\mathrm{T}}+\left\|\rho^n-G^n\right\|_{\mathrm{T}}\leq C\left(\Delta t^2+h^2\right), \tag{45}$$

where C is a positive constant independent of Δt and h.

Proof. Noticing that

$$\left\|U^0\right\|_\infty=\left\|u^0\right\|_{L^\infty([a,b])}\leq L,$$

and from Theorem 3.1, we can easily get the boundedness of the numerical solution U^1 by using the triangle inequality and inverse inequality, i.e.,

$$\left\|U^1\right\|_\infty\leq\left\|U^1-u^1\right\|_\infty+\left\|u^1\right\|_{L^\infty([a,b])}\leq Ch^{-1/2}\left(\Delta t^2+h^2\right)+L\leq L+1, \tag{46}$$

under the time stepsize ratio restriction $\Delta t=o(h^{1/4})$.

We now assume (44) holds for all $k\leq n-1$ with $n\geq 2$. We need to prove that (44)–(45) also hold for $k=n$. The exact solutions u_i^n, $\rho_{i+1/2}^n$ and $p_{i+1/2}^n$ of (5)–(7) can be written into a similar formats as the linearized BDF2-BCFD scheme (11)–(13), that is

$$\begin{aligned}
&D_t(u+\eta)_i^n+D_t[D_hp_i^n]+D_h\rho_i^n-u_i^{n,*}\bar{p}_i^n\\
&\qquad=S_{1,i}^n-S_{2,i}^n+\omega_i^n,\quad i=1,\ldots,M,
\end{aligned} \tag{47}$$

$$D_t\rho_{i+1/2}^n-p_{i+1/2}^n=S_{3,i+1/2}^n,\quad i=1,\ldots,M-1, \tag{48}$$

$$p_{i+1/2}^n+d_h(u+\eta)_{i+1/2}^n=\xi_{i+1/2}^n,\quad i=1,\ldots,M-1, \tag{49}$$

$$\rho_{1/2}^n = \rho_{M+1/2}^n = 0, \quad p_{1/2}^n = p_{M+1/2}^n = 0, \tag{50}$$

where, for $n \geq 2$, the truncation errors

$$\begin{aligned}
S_{1,i}^n &= D_t u_i^n - (u_t)_i^n + D_t[D_h p_i^n] - (p_{xt})_i^n + D_h \rho_i^n - (\rho_x)_i^n, \\
S_{2,i}^n &= u_i^{n,*} \bar{p}_i^n - [up]_i^n, \\
S_{3,i+1/2}^n &= D_t \rho_{i+1/2}^n - (\rho_t)_{i+1/2}^n,
\end{aligned}$$

and ω^n and ξ^n are defined respectively by (25) and (28), and estimated by (26) and Lemma 3.1. Moreover, by using the Taylor expansion, the truncation errors can also be estimated as:

$$\begin{aligned}
|S_{1,i}^n| &\leq C\Delta t^2 \left(\|u_{ttt}\|_{L^\infty(\bar{Q})} + \|p_{xttt}\|_{L^\infty(\bar{Q})} + \|\rho_{xtt}\|_{L^\infty(\bar{Q})} \right) \\
&\quad + Ch^2 \left(\|p_{xxxt}\|_{L^\infty(\bar{Q})} + \|\rho_{xxx}\|_{L^\infty(\bar{Q})} \right) = \mathcal{O}(\Delta t^2 + h^2), \\
|S_{2,i}^n| &\leq C \left(\Delta t^2 \|up_{tt}\|_{L^\infty(\bar{Q})} + h^2 \|up_{xx}\|_{L^\infty(\bar{Q})} + \Delta t^2 \|u_t p\|_{L^\infty(\bar{Q})} \right) \\
&= \mathcal{O}(\Delta t^2 + \ h^2), \\
|S_{3,i-1/2}^n| &\leq C\Delta t^2 \left(\|\rho_{ttt}\|_{L^\infty(\bar{Q})} + \|p_{tt}\|_{L^\infty(\bar{Q})} \right) = \mathcal{O}(\Delta t^2),
\end{aligned}$$

and thus, similar to (33), we have

$$\|S_1^n\|_{\mathrm{M}} = \mathcal{O}(\Delta t^2 + h^2), \quad \|S_2^n\|_{\mathrm{M}} = \mathcal{O}(\Delta t^2 + h^2), \quad \|S_3^n\|_{\mathrm{T}} = \mathcal{O}(\Delta t^2). \tag{51}$$

Let $\iota_i^n := u_i^{n,*} \bar{p}_i^n - U_i^{n,*} \bar{P}_i^n$. Then, by subtracting (11)–(13) from (47)–(49), we derive the error equations

$$\begin{aligned}
&D_t(\theta + \eta)_i^n + D_t[D_h \mu_i^n] + D_h \lambda_i^n - \iota_i^n \\
&\qquad = S_{1,i}^n - S_{2,i}^n + \omega_i^n, \quad i = 1, \ldots, M, \qquad (52) \\
&D_t \lambda_{i+1/2}^n - \mu_{i+1/2}^n = S_{3,i+1/2}^n, \quad i = 1, \ldots, M-1, \qquad (53) \\
&\mu_{i+1/2}^n + [d_h(\theta + \eta)]_{i+1/2}^n = \xi_{i+1/2}^n, \quad i = 1, \ldots, M-1, \qquad (54) \\
&\lambda_{1/2}^n = \lambda_{M+1/2}^n = 0, \quad \mu_{1/2}^n = \mu_{M+1/2}^n = 0. \qquad (55)
\end{aligned}$$

Now, taking discrete inner products with $\theta^n + \eta^n$, λ^n and $D_t \mu^n$ for (52), (53) and (54), respectively, we get

$$\begin{aligned}
&\left(D_t\left(\theta^n + \eta^n\right), \theta^n + \eta^n\right)_{\mathrm{M}} + \left(D_t\left[D_h \mu^n\right], \theta^n + \eta^n\right)_{\mathrm{M}} + \left(D_h \lambda^n, \theta^n + \eta^n\right)_{\mathrm{M}} \\
&\qquad - \left(\iota^n, \theta^n + \eta^n\right)_{\mathrm{M}} = \left(S_1^n - S_2^n, \theta^n + \eta^n\right)_{\mathrm{M}} + \left(\omega^n, \theta^n + \eta^n\right)_{\mathrm{M}}, \qquad (56) \\
&\left(D_t \lambda^n, \lambda^n\right)_{\mathrm{T}} - \left(\mu^n, \lambda^n\right)_{\mathrm{T}} = \left(S_3^n, \lambda^n\right)_{\mathrm{T}}, \qquad (57) \\
&\left(D_t \mu^n, \mu^n\right)_{\mathrm{M}} + \left(d_h(\theta + \eta)^n, D_t \mu^n\right)_{\mathrm{T}} = \left(\xi^n, D_t \mu^n\right)_{\mathrm{T}}. \qquad (58)
\end{aligned}$$

Similar as the proof of Theorem 3.1, by adding (56)–(58) together, and utilizing the facts that

$$\begin{aligned}
\left(D_t\left[D_h \mu^n\right], \theta^n + \eta^n\right)_{\mathrm{M}} &= -\left(d_h(\theta + \eta)^n, D_t \mu^n\right)_{\mathrm{T}}, \\
\left(D_h \lambda^n, \theta^n + \eta^n\right)_{\mathrm{M}} &= -\left(d_h(\theta + \eta)^n, \lambda^n\right)_{\mathrm{T}} = \left(\mu^n, \lambda^n\right)_{\mathrm{T}} - \left(\xi^n, \lambda^n\right)_{\mathrm{T}},
\end{aligned}$$

we obtain

$$\begin{aligned}
&\left(D_t\left(\theta^n + \eta^n\right), \theta^n + \eta^n\right)_{\mathrm{M}} + \left(D_t \mu^n, \mu^n\right)_{\mathrm{T}} + \left(D_t \lambda^n, \lambda^n\right)_{\mathrm{T}} \\
&\quad = \left(\iota^n, \theta^n + \eta^n\right)_{\mathrm{M}} + \left(S_1^n - S_2^n, \theta^n + \eta^n\right)_{\mathrm{M}} + \left(\omega^n, \theta^n + \eta^n\right)_{\mathrm{M}} + \left(\xi^n, \lambda^n\right)_{\mathrm{T}} \qquad (59) \\
&\qquad + \left(S_3^n, \lambda^n\right)_{\mathrm{T}} + \left(\xi^n, D_t \mu^n\right)_{\mathrm{T}}.
\end{aligned}$$

Next, we first estimate the left-hand side of (59). Noting that for any $a, b, c \in \mathbb{R}$,

$$(3a-4b+c)\,a = \frac{1}{2}\left[a^2+(2a-b)^2\right] - \frac{1}{2}\left[b^2+(2b-c)^2\right] + \frac{1}{2}(a-2b+c)^2.$$

Then, the terms on left-hand side of (59) can be bounded from below by

$$\begin{aligned}(60)\qquad &\left(D_t\left(\theta+\eta\right)^n, \left(\theta+\eta\right)^n\right)_{\mathrm{M}} + \left(D_t\mu^n, \mu^n\right)_{\mathrm{T}} + \left(D_t\lambda^n, \lambda^n\right)_{\mathrm{T}} \\ &\quad \geq \frac{1}{4\Delta t}\left[(E^n)^2 - (E^{n-1})^2\right],\end{aligned}$$

where

$$\begin{aligned}(E^n)^2 := &\left(\|(\theta+\eta)^n\|_{\mathrm{M}}^2 + \left\|2(\theta+\eta)^n - (\theta+\eta)^{n-1}\right\|_{\mathrm{M}}^2\right) \\ &+ \left(\|\mu^n\|_{\mathrm{T}}^2 + \left\|2\mu^n - \mu^{n-1}\right\|_{\mathrm{T}}^2\right) + \left(\|\lambda^n\|_{\mathrm{T}}^2 + \left\|2\lambda^n - \lambda^{n-1}\right\|_{\mathrm{T}}^2\right).\end{aligned}$$

Second, we analyze the right-hand side of (59). From the definition of ι^n and Lemma 2.2, we obtain

$$\|\iota^n\|_{\mathrm{M}} = \left\|\left(u^{n,*} - U^{n,*}\right)\bar{p}^n + U^{n,*}\left(\bar{p}^n - \bar{P}^n\right)\right\|_{\mathrm{M}} \leq C\left[\left\|2\theta^{n-1} - \theta^{n-2}\right\|_{\mathrm{M}} + \|\mu^n\|_{\mathrm{T}}\right],$$

where assumption (44) is utilized to bound $\|U^{n,*}\|_\infty$. Therefore, the first term of the right-hand side can be estimated by

$$\begin{aligned}(61)\qquad \left(\iota^n, \theta^n+\eta^n\right)_{\mathrm{M}} &\leq \|\iota^n\|_{\mathrm{M}}\left\|(\theta+\eta)^n\right\|_{\mathrm{M}} \\ &\leq C\left[\left\|2\theta^{n-1} - \theta^{n-2}\right\|_{\mathrm{M}}^2 + \|\mu^n\|_{\mathrm{T}}^2 + \|(\theta+\eta)^n\|_{\mathrm{M}}^2\right].\end{aligned}$$

For the second to fifth terms on the right-hand side of (59), we directly have

$$(62)\qquad \left|\left(S_1^n - S_2^n, \theta^n+\eta^n\right)_{\mathrm{M}}\right| \leq C\left(\|S_1^n\|_{\mathrm{M}}^2 + \|S_2^n\|_{\mathrm{M}}^2 + \|(\theta+\eta)^n\|_{\mathrm{M}}^2\right),$$

$$(63)\qquad \left|\left(\omega^n, \theta^n+\eta^n\right)_{\mathrm{M}}\right| \leq C\left(\|\omega^n\|_{\mathrm{M}}^2 + \|(\theta+\eta)^n\|_{\mathrm{M}}^2\right),$$

$$(64)\qquad \left|\left(\xi^n, \lambda^n\right)_{\mathrm{T}}\right| \leq C\left(\|\xi^n\|_{\mathrm{T}}^2 + \|\lambda^n\|_{\mathrm{T}}^2\right),$$

$$(65)\qquad \left|\left(S_3^n, \lambda^n\right)_{\mathrm{T}}\right| \leq C\left(\|S_3^n\|_{\mathrm{T}}^2 + \|\lambda^n\|_{\mathrm{T}}^2\right).$$

Inserting (60)–(65) into (59), then multiplying the resulting equation by Δt, and summing over k from 2 to n, we obtain

$$\begin{aligned}(66)\qquad (E^n)^2 \leq (E^1)^2 + C\max_{2\leq k\leq n}&\left[\left\|S_1^k\right\|_{\mathrm{M}}^2 + \left\|S_2^k\right\|_{\mathrm{M}}^2 + \left\|S_3^k\right\|_{\mathrm{T}}^2 + \left\|\omega^k\right\|_{\mathrm{M}}^2 + \left\|\xi^k\right\|_{\mathrm{T}}^2\right. \\ &\left. + \left\|\eta^k\right\|_{\mathrm{M}}^2\right] + C\sum_{k=2}^{n}\Delta t\left(E^k\right)^2 + \sum_{k=2}^{n}\Delta t\left(D_t\mu^k, \xi^k\right)_{\mathrm{T}}.\end{aligned}$$

While the last term in (66) requires a lot of careful consideration. By applying summation by parts, we see

$$\begin{aligned}\sum_{k=2}^{n}\Delta t\left(D_t\mu^k, \xi^k\right)_{\mathrm{T}} = &\sum_{k=1}^{n-2}\Delta t\left(\mu^k, \hat{D}_t\xi^k\right)_{\mathrm{T}} - \frac{3}{2}\left(\mu^1, \xi^1\right)_{\mathrm{T}} - \frac{3\Delta t}{2}\left(\mu^{n-1}, \delta_t\xi^n\right)_{\mathrm{T}} \\ &+ \frac{1}{2}\left(\mu^n, \xi^n\right)_{\mathrm{T}} + \frac{1}{2}\left(2\mu^n - \mu^{n-1}, \xi^n\right)_{\mathrm{T}}.\end{aligned}$$

Then, Young's inequality implies that

$$\begin{aligned}\left|\sum_{k=2}^{n}\Delta t\ \left(D_t\mu^k,\xi^k\right)_{\mathrm{T}}\right| &\le C\sum_{k=1}^{n-1}\Delta t\left[\left\|\mu^k\right\|_{\mathrm{T}}^2+\left\|\hat{D}_t\xi^k\right\|_{\mathrm{T}}^2\right]\\ &\quad+C\left[\Delta t\left\|\delta_t\xi^n\right\|_{\mathrm{T}}^2+\left\|\mu^1\right\|_{\mathrm{T}}^2+\left\|\xi^1\right\|_{\mathrm{T}}^2\right]\\ &\quad+C\left\|\xi^n\right\|_{\mathrm{T}}^2+\epsilon\left[\left\|\mu^n\right\|_{\mathrm{T}}^2+\left\|2\mu^n-\mu^{n-1}\right\|_{\mathrm{T}}^2\right],\end{aligned}\tag{67}$$

where ϵ is a sufficiently small positive constant. Substituting (67) into (66), we obtain

$$\begin{aligned}(E^n)^2 &\le C\left(\left\|(\theta+\eta)^1\right\|_{\mathrm{M}}^2+\left\|\eta^0\right\|_{\mathrm{M}}^2+\left\|\mu^1\right\|_{\mathrm{T}}^2+\left\|\lambda^1\right\|_{\mathrm{T}}^2+\left\|\xi^1\right\|_{\mathrm{T}}^2\right)\\ &\quad+C\max_{2\le k\le n}\left[\left\|S_1^k\right\|_{\mathrm{M}}^2+\left\|S_2^k\right\|_{\mathrm{M}}^2+\left\|S_3^k\right\|_{\mathrm{T}}^2+\left\|\omega^k\right\|_{\mathrm{M}}^2+\left\|\xi^k\right\|_{\mathrm{T}}^2\right.\\ &\quad\left.+\left\|\hat{D}_t\xi^{k-1}\right\|_{\mathrm{T}}^2+\left\|\eta^k\right\|_{\mathrm{M}}^2\right]+C\Delta t\left\|\delta_t\xi^n\right\|_{\mathrm{T}}^2+C\sum_{k=1}^{n}\Delta t\,(E^k)^2.\end{aligned}\tag{68}$$

Thus, for sufficiently small Δt, application of discrete Grönwall's inequality to (68), and estimates (26), (43), (51) and Lemma 3.1 directly imply that

$$\left\|\theta^n+\eta^n\right\|_{\mathrm{M}}+\left\|\mu^n\right\|_{\mathrm{T}}^2+\left\|\lambda^n\right\|_{\mathrm{T}}^2\le(E^n)^2\le C\left(\Delta t^2+h^2\right),$$

which proves (45) for $k=n$.

Finally, analogous to the process (46), we can easily prove the boundedness of the numerical solution U^n:

$$\left\|U^n\right\|_\infty\le\left\|U^n-u^n\right\|_\infty+\left\|u^n\right\|_{L^\infty([a,b])}\le Ch^{-1/2}\left(\Delta t^2+h^2\right)+L\le L+1,$$

under condition $\Delta t=o(h^{1/4})$. Thus, the proof of Theorem 3.2 is completed. □

3.2. Error estimate of the linearized CN-BCFD scheme. Analysis of the CN-BCFD scheme (19)–(21) follows basically the same line as the BDF2-BCFD scheme (11)–(13). Noting that the exact solutions u_i^n, $p_{i+1/2}^n$ and $\rho_{i+1/2}^n$ for $n\ge1$ of (5)–(7) satisfy a similar format of (19)–(21) that

$$\begin{aligned}&\delta_t(u+\eta)_i^n+\delta_t[D_hp_i^n]+D_h\hat{\rho}_i^{n-1/2}-u_i^{n,\star}\hat{p}_i^{n-1/2}\\ &\qquad=Z_{1,i}^{n-1/2}+\tilde{\omega}_i^n,\quad i=1,\dots,M,\end{aligned}\tag{69}$$

$$\delta_t\rho_{i+1/2}^n-\hat{p}_{i+1/2}^{n-1/2}=Z_{2,i+1/2}^{n-1/2},\quad i=1,\dots,M-1,\tag{70}$$

$$p_{i+1/2}^n+d_h(u+\eta)_{i+1/2}^n=\xi_{i+1/2}^n,\quad i=1,\dots,M-1,\tag{71}$$

$$\rho_{1/2}^n=\rho_{M+1/2}^n=0,\quad p_{1/2}^n=p_{M+1/2}^n=0,\tag{72}$$

where

$$\begin{aligned}Z_{1,i}^{n-1/2}&=\delta_tu_i^n-[u_t]_i^{n-1/2}+\delta_t[D_hp_i^n]-[p_{xt}]_i^{n-1/2}+D_h\hat{\rho}_i^{n-1/2}-[\rho_x]_i^{n-1/2}\\ &\quad-\left(u_i^{n,\star}\hat{p}_i^{n-1/2}-[up]_i^{n-1/2}\right),\\ Z_{2,i+1/2}^{n-1/2}&=\delta_t\rho_{i+1/2}^n-[\rho_t]_{i+1/2}^{n-1/2}-\left(\hat{p}_{i+1/2}^{n-1/2}-p_{i+1/2}^{n-1/2}\right).\end{aligned}$$

and $\tilde{\omega}^n$ and ξ^n are estimated by (27) and Lemma 3.1. Similar to (33) and (51), the truncation errors can be easily estimated by using the Taylor expansion:

$$\left\|Z_1^{n-1/2}\right\|_{\mathrm{M}}=\begin{cases}\mathcal{O}(\Delta t+h^2), & n=1,\\ \mathcal{O}(\Delta t^2+h^2), & n\ge2;\end{cases}\qquad\left\|Z_2^{n-1/2}\right\|_{\mathrm{T}}=\mathcal{O}(\Delta t^2),\ n\ge1.$$

Theorem 3.3. *Assume that (22) holds, for $n \geq 1$, under a time stepsize ratio restriction $\Delta t = o(h^{1/4})$, we have*

$$\|U^n\|_\infty \leq L + 1, \tag{73}$$

and

$$\|u^n - U^n\|_{\mathrm{M}} + \|p^n - P^n\|_{\mathrm{T}} + \|\rho^n - G^n\|_{\mathrm{T}} \leq C\left(\Delta t^2 + h^2\right), \tag{74}$$

where C is a positive constant independent of Δt and h.

Proof. It follows from Theorem 3.1 that (74) holds for $n = 1$, and $\left\|U^1\right\|_\infty \leq C$ under condition $\Delta t = o(h^{1/4})$, see (46).

Now, we assume $\left\|U^k\right\|_\infty \leq C$, $k \leq n-1$ with $n \geq 2$, and we shall prove that (73)–(74) also hold for $k = n$. Let $\kappa_i^{n-1/2} := u_i^{n,\star}\hat{\bar{p}}_i^{n-1/2} - U_i^{n,\star}\hat{\bar{P}}_i^{n-1/2}$ for $n \geq 2$. It is easy to check that

$$\begin{aligned}\left\|\kappa^{n-1/2}\right\|_{\mathrm{M}} &= \left\|\left(u^{n,\star} - U^{n,\star}\right)\hat{\bar{p}}_i^{n-1/2} + U^{n,\star}\left(\hat{\bar{p}}_i^{n-1/2} - \hat{\bar{P}}_i^{n-1/2}\right)\right\|_{\mathrm{M}} \\ &\leq C\left[\left\|\theta^{n-1}\right\|_{\mathrm{M}} + \left\|\theta^{n-2}\right\|_{\mathrm{M}} + \|\mu^n\|_{\mathrm{T}} + \left\|\mu^{n-1}\right\|_{\mathrm{T}}\right],\end{aligned}$$

where Lemma 2.2 and the boundedness of $\|U^{n,\star}\|_\infty$ are utilized.

By subtracting (19)–(21) from (69)–(71), we have the error equations

$$\begin{aligned}&\delta_t(\theta+\eta)_i^n + \delta_t[D_h\mu_i^n] + D_h\hat{\lambda}_i^{n-1/2} - \kappa_i^{n-1/2} \\ &\qquad = Z_{1,i}^{n-1/2} + \tilde{\omega}_i^n, \quad i = 1, \ldots, M,\end{aligned} \tag{75}$$

$$\delta_t\lambda_{i+1/2}^n - \hat{\mu}_{i+1/2}^{n-1/2} = Z_{2,i+1/2}^{n-1/2}, \quad i = 1, \ldots, M-1, \tag{76}$$

$$\mu_{i+1/2}^n + d_h(\theta+\eta)_{i+1/2}^n = \xi_{i+1/2}^n, \quad i = 1, \ldots, M-1, \tag{77}$$

$$\lambda_{1/2}^n = \lambda_{M+1/2}^n = 0, \quad \mu_{1/2}^n = \mu_{M+1/2}^n = 0. \tag{78}$$

Adding (77) at time levels t^n and t^{n-1}, we obtain

$$\hat{\mu}_{i+1/2}^{n-1/2} + d_h(\hat{\theta}+\hat{\eta})_{i+1/2}^{n-1/2} = \hat{\xi}_{i+1/2}^{n-1/2}, \quad i = 1, \ldots, M-1; \quad \hat{\mu}_{1/2}^{n-1/2} = \hat{\mu}_{M+1/2}^{n-1/2} = 0. \tag{79}$$

Next, taking discrete inner products with $(\hat{\theta}+\hat{\eta})^{n-1/2}$, $\hat{\lambda}^{n-1/2}$ and $\delta_t\mu^n$, respectively, for (75), (76) and (79). Then, analogous to the proof of Theorems 3.1 and 3.2, by adding the three resulting equations together, and multiplying it by Δt and summing over k from 2 to n, we obtain by standard Cauchy-Schwartz inequality that

$$\begin{aligned}&\|(\theta+\eta)^n\|_{\mathrm{M}}^2 + \|\mu^n\|_{\mathrm{T}}^2 + \|\lambda^n\|_{\mathrm{T}}^2 \\ &\leq \left\|(\theta+\eta)^1\right\|_{\mathrm{M}}^2 + \left\|\mu^1\right\|_{\mathrm{T}}^2 + \left\|\lambda^1\right\|_{\mathrm{T}}^2 \\ &\quad + C\max_{2\leq k\leq n}\left[\left\|Z_1^{k-1/2}\right\|_{\mathrm{M}}^2 + \left\|Z_2^{k-1/2}\right\|_{\mathrm{T}}^2 + \left\|\tilde{\omega}^k\right\|_{\mathrm{M}}^2 + \left\|\xi^k\right\|_{\mathrm{T}}^2 + \left\|\eta^k\right\|_{\mathrm{M}}^2\right] \\ &\quad + C\sum_{k=1}^n \Delta t\left[\left\|(\theta+\eta)^k\right\|_{\mathrm{M}}^2 + \left\|\mu^k\right\|_{\mathrm{T}}^2 + \left\|\lambda^k\right\|_{\mathrm{T}}^2\right] + \sum_{k=2}^n \Delta t\left(\delta_t\mu^k, \hat{\xi}^{k-1/2}\right)_{\mathrm{T}},\end{aligned} \tag{80}$$

where we have utilized the facts that

$$\left(\delta_t\left[D_h\mu^n\right], (\hat{\theta}+\hat{\eta})^{n-1/2}\right)_{\mathrm{M}} = -\left(d_h(\hat{\theta}+\hat{\eta})^{n-1/2}, \delta_t\mu^n\right)_{\mathrm{T}},$$

$$\left(D_h\hat{\lambda}^{n-1/2}, (\hat{\theta}+\hat{\eta})^{n-1/2}\right)_{\mathrm{M}} = \left(\hat{\mu}^{n-1/2}, \lambda^n\right)_{\mathrm{T}} - \left(\hat{\xi}^{n-1/2}, \hat{\lambda}^{n-1/2}\right)_{\mathrm{T}},$$

$$\left(\delta_t\left(\theta^n+\eta^n\right),(\hat{\theta}+\hat{\eta})^{n-1/2}\right)_{\mathrm{M}}+\left(\delta_t\mu^n,\hat{\mu}^{n-1/2}\right)_{\mathrm{T}}+\left(\delta_t\lambda^n,\hat{\lambda}^{n-1/2}\right)_{\mathrm{T}}$$
$$=\frac{1}{2\Delta t}\left(\|(\theta+\eta)^n\|_{\mathrm{M}}^2+\|\mu^n\|_{\mathrm{T}}^2+\|\lambda^n\|_{\mathrm{T}}^2-\|(\theta+\eta)^{n-1}\|_{\mathrm{M}}^2-\|\mu^{n-1}\|_{\mathrm{T}}^2-\|\lambda^{n-1}\|_{\mathrm{T}}^2\right).$$

We also have to pay special attention to the last term of the right-hand side of (80). By summation by parts and Young's inequality we have

(81)
$$\begin{aligned}
&\sum_{k=2}^{n}\Delta t\left(\delta_t\mu^k,\hat{\xi}^{k-1/2}\right)_{\mathrm{T}}\\
&=-\sum_{k=2}^{n-1}\frac{\Delta t}{2}\left(\mu^k,\delta_t\xi^k\right)_{\mathrm{T}}-\sum_{k=3}^{n}\frac{\Delta t}{2}\left(\mu^{k-1},\delta_t\xi^k\right)_{\mathrm{T}}+\left(\mu^1,\hat{\xi}^{3/2}\right)_{\mathrm{T}}+\left(\mu^n,\hat{\xi}^{n-1/2}\right)_{\mathrm{T}}\\
&\le C\sum_{k=2}^{n-1}\Delta t\left\|\mu^k\right\|_{\mathrm{T}}^2+C\sum_{k=2}^{n}\Delta t\left\|\delta_t\xi^k\right\|_{\mathrm{T}}^2+\frac{1}{2}\left(\|\mu^1\|_{\mathrm{T}}^2+\|\mu^n\|_{\mathrm{T}}^2\right)\\
&\quad+C\left(\|\xi^1\|_{\mathrm{T}}^2+\|\xi^2\|_{\mathrm{T}}^2+\|\xi^n\|_{\mathrm{T}}^2+\|\xi^{n-1}\|_{\mathrm{T}}^2\right).
\end{aligned}$$

Then, inserting (81) into (80), following the same line of proof for Theorem 3.2, applying the known results in (24), (27), Lemma 3.1 and Theorem 3.1, one can easily get the results (74) and thus (73) for $k=n$ under condition $\Delta t=o(h^{1/4})$. Therefore, the proof is finished. □

4. Stability for the linearized BCFD schemes

With the help of the preceding three theorems about convergence in Section 3, we are now in the position to prove the stability of the proposed BCFD schemes for the initial-boundary value problem (1)–(2), which theoretically support the feasibility of long-time simulations of solitons.

To begin with, it is sure that the stability of the first time level scheme (14)–(16) shall be considered.

Theorem 4.1. *Let* $\left\{U^1,P^1,G^1\right\}$ *be the solution of* (14)–(16). *Then, we have*

$$\left\|U^1\right\|_{\mathrm{M}}+\left\|P^1\right\|_{\mathrm{T}}+\left\|G^1\right\|_{\mathrm{T}}\le C\left(\left\|U^0\right\|_{\mathrm{M}}+\left\|P^0\right\|_{\mathrm{T}}+\left\|G^0\right\|_{\mathrm{T}}\right), \tag{82}$$

where C *is a positive constant independent of* Δt *and* h.

Proof. Recalling the first time level scheme (14)–(16), by taking discrete inner products with U^1 and G^1, respectively, for (14) and (15), it follows that

$$\left(\delta_tU^1,U^1\right)_{\mathrm{M}}+\left(\delta_t[D_hP^1],U^1\right)_{\mathrm{M}}+\left(D_h\hat{G}^{1/2},U^1\right)_{\mathrm{M}}-\left(U^0\hat{\bar{P}}^{1/2},U^1\right)_{\mathrm{M}}=0, \tag{83}$$

$$\left(\delta_tG^1,G^1\right)_{\mathrm{T}}-\left(\hat{P}^{1/2},G^1\right)_{\mathrm{T}}=0. \tag{84}$$

Moreover, according to Lemma 2.1, and utilizing the equations (16) and (84), we have

$$\begin{aligned}
\left(\delta_t[D_hP^1],U^1\right)_{\mathrm{M}}&=-\left(d_hU^1,\delta_tP^1\right)_{\mathrm{T}}=\left(P^1,\delta_tP^1\right)_{\mathrm{T}},\\
\left(D_h\hat{G}^{1/2},U^1\right)_{\mathrm{M}}&=-\left(d_hU^1,\hat{G}^{1/2}\right)_{\mathrm{T}}=\left(P^1,\hat{G}^{1/2}\right)_{\mathrm{T}}\\
&=\left(\delta_tG^1,G^1\right)_{\mathrm{T}}-\frac{1}{2}\left(P^0,G^1\right)_{\mathrm{T}}+\frac{1}{2}\left(P^1,G^0\right)_{\mathrm{T}}.
\end{aligned} \tag{85}$$

Then, inserting (85) into (83), and noting the fact

$$\begin{aligned}&\left(\delta_t U^1, U^1\right)_{\mathrm{M}}+\left(\delta_t P^1, P^1\right)_{\mathrm{T}}+\left(\delta_t G^1, G^1\right)_{\mathrm{T}}\\&=\frac{1}{\Delta t}\left(\left\|U^1\right\|_{\mathrm{M}}^2+\left\|P^1\right\|_{\mathrm{T}}^2+\left\|G^1\right\|_{\mathrm{T}}^2-\left(U^0, U^1\right)_{\mathrm{M}}-\left(P^0, P^1\right)_{\mathrm{T}}-\left(G^0, G^1\right)_{\mathrm{T}}\right),\end{aligned}$$

we immediately get

$$\begin{aligned}&\left\|U^1\right\|_{\mathrm{M}}^2+\left\|P^1\right\|_{\mathrm{T}}^2+\left\|G^1\right\|_{\mathrm{T}}^2\\&=\left(U^0, U^1\right)_{\mathrm{M}}+\left(P^0, P^1\right)_{\mathrm{T}}+\left(G^0, G^1\right)_{\mathrm{T}}\\&\quad+\frac{\Delta t}{2}\left[\left(P^0, G^1\right)_{\mathrm{T}}-\left(P^1, G^0\right)_{\mathrm{T}}+2\left(U^0 \hat{P}^{1/2}, U^1\right)_{\mathrm{M}}\right].\end{aligned}\tag{86}$$

Therefore, application of Cauchy-Schwartz inequality and the fact that $\left\|U^0\right\|_{\infty} \leq L$, we obtain

$$\begin{aligned}&\left\|U^1\right\|_{\mathrm{M}}^2+\left\|P^1\right\|_{\mathrm{T}}^2+\left\|G^1\right\|_{\mathrm{T}}^2\\&\leq\left(\frac{1}{2}+\frac{(1+2L)\Delta t}{4}\right)\left(\|U^1\|_{\mathrm{M}}^2+\|P^1\|_{\mathrm{T}}^2+\|G^1\|_{\mathrm{T}}^2+\|U^0\|_{\mathrm{M}}^2+\|P^0\|_{\mathrm{T}}^2+\|G^0\|_{\mathrm{T}}^2\right).\end{aligned}\tag{87}$$

If Δt is sufficiently small, see, $\Delta t \leq \frac{1}{1+2L}$, we can directly get the conclusion (82). □

Based on the above theorem, we now turn to prove the stability of the linearized BDF2-BCFD scheme (11)–(13) for $n \geq 2$.

Theorem 4.2. *Assume that (22) holds. For the numerical solution $\{U^n, P^n, G^n\}$ of the linearized BDF2-BCFD scheme (11)–(13), under time stepsize ratio restriction $\Delta t = o(h^{1/4})$, we have*

$$\|U^n\|_{\mathrm{M}}+\|P^n\|_{\mathrm{T}}+\|G^n\|_{\mathrm{T}} \leq C\left(\left\|U^0\right\|_{\mathrm{M}}+\left\|P^0\right\|_{\mathrm{T}}+\left\|G^0\right\|_{\mathrm{T}}\right),$$

where C is a positive constant independent of Δt and h.

Proof. Similar as the convergence proof in Theorem 3.2, by taking discrete inner products with U^n, G^n and $D_t P^n$ for (11), (12) and (13), respectively, we get

$$\left(D_t U^n, U^n\right)_{\mathrm{M}}+\left(D_t[D_h P^n], U^n\right)_{\mathrm{M}}+\left(D_h G^n, U^n\right)_{\mathrm{M}}=\left(U^{n,*} \bar{P}^n, U^n\right)_{\mathrm{M}},\tag{88}$$

$$\left(D_t G^n, G^n\right)_{\mathrm{T}}-\left(P^n, G^n\right)_{\mathrm{T}}=0,\tag{89}$$

$$\left(P^n, D_t P^n\right)_{\mathrm{T}}+\left(d_h U^n, D_t P^n\right)_{\mathrm{T}}=0.\tag{90}$$

Then, adding the three equations (88)–(90) together, multiplying it by $4\Delta t$ and summing over k from 2 to n, and using the boundedness of the numerical solution proved in Theorem 3.2, we obtain by standard Cauchy-Schwartz inequality that

$$\begin{aligned}&\|U^n\|_{\mathrm{M}}^2+\left\|2U^n-U^{n-1}\right\|_{\mathrm{M}}^2+\|P^n\|_{\mathrm{T}}^2+\left\|2P^n-P^{n-1}\right\|_{\mathrm{T}}^2+\|G^n\|_{\mathrm{T}}^2+\left\|2G^n-G^{n-1}\right\|_{\mathrm{T}}^2\\&=:\Theta^n \leq \Theta^1+C\sum_{k=2}^{n}\Delta t\left(\left\|U^k\right\|_{\mathrm{M}}^2+\left\|P^k\right\|_{\mathrm{T}}^2\right) \leq \Theta^1+C\sum_{k=2}^{n}\Delta t\,\Theta^k,\end{aligned}\tag{91}$$

where we have also utilized the facts that

$$\begin{aligned}\left(D_t[D_h P^n], U^n\right)_{\mathrm{M}}&=-\left(d_h U^n, D_t P^n\right)_{\mathrm{T}},\\\left(D_h G^n, U^n\right)_{\mathrm{M}}&=-\left(d_h U^n, G^n\right)_{\mathrm{T}}=\left(P^n, G^n\right)_{\mathrm{T}},\\\left(D_t U^n, U^n\right)_{\mathrm{M}}+\left(D_t P^n, P^n\right)_{\mathrm{T}}+\left(D_t G^n, G^n\right)_{\mathrm{T}}&\geq\frac{1}{4\Delta t}\left[(\Theta^n)^2-(\Theta^{n-1})^2\right].\end{aligned}$$

Finally, for sufficiently small Δt, we apply the discrete Grönwall's inequality to (91), and using the result of Theorem 4.1 and the triangle inequality, we obtain

$$\begin{aligned}&\|U^n\|_{\mathrm{M}} + \|P^n\|_{\mathrm{T}} + \|G^n\|_{\mathrm{T}}\\ &\le C\left(\left\|U^1\right\|_{\mathrm{M}} + \left\|P^1\right\|_{\mathrm{T}} + \left\|G^1\right\|_{\mathrm{T}} + \left\|U^0\right\|_{\mathrm{M}} + \left\|P^0\right\|_{\mathrm{T}} + \left\|G^0\right\|_{\mathrm{T}}\right)\\ &\le C\left(\left\|U^0\right\|_{\mathrm{M}} + \left\|P^0\right\|_{\mathrm{T}} + \left\|G^0\right\|_{\mathrm{T}}\right),\end{aligned}$$

which proves Theorem 4.2. □

Similarly, using the same arguments as in the convergence proof of Theorem 3.3, and noting the boundedness of the numerical solution, we can easily carry out the stability proof for the linearized CN-BCFD scheme (19)–(21).

Theorem 4.3. *Assume that (22) holds. For the numerical solution $\{U^n, P^n, G^n\}$ of the linearized CN-BCFD scheme (19)–(21), under time stepsize ratio restriction $\Delta t = o(h^{1/4})$, we have*

$$\|U^n\|_{\mathrm{M}} + \|P^n\|_{\mathrm{T}} + \|G^n\|_{\mathrm{T}} \le C\left(\left\|U^0\right\|_{\mathrm{M}} + \left\|P^0\right\|_{\mathrm{T}} + \left\|G^0\right\|_{\mathrm{T}}\right),$$

where C is a positive constant independent of Δt and h.

Remark 4.1. The stability conclusions of Theorems 4.2 and 4.3 can be viewed as discrete versions of the following continuous stability result:

(92)
$$\int_I \left(u^2(x,t) + u_x^2(x,t) + \rho^2(x,t)\right) dx \le \exp(tL) \int_I \left(u^2(x,0) + u_x^2(x,0) + \rho^2(x,0)\right) dx,$$

which can be proved by taking inner products with u and ρ respectively for problem (1)–(2) under assumption (23).

Remark 4.2. The stability conclusions of Theorems 4.2 and 4.3 imply that the homogeneous BDF2-BCFD scheme (11)–(13) and homogeneous CN-BCFD scheme (19)–(21) only have trivial solutions, which show the uniqueness of solutions. Moreover, since the two schemes are both linear, existence is thus equivalent to the uniqueness, which directly show the existence of solutions.

5. Numerical experiment

In this section, some numerical experiments using the linearized BDF2-BCFD algorithm (11)–(13) and linearized CN-BCFD algorithm (19)–(21) are carried out. Both uniform and non-uniform spatial grids are considered. To show the efficiency of our linearized method, a fully nonlinear method (cf. [31]) with homogeneous Dirichlet boundary condition on uniform spatial grids is introduced:

$$\begin{aligned}&\delta_t U_i^n + \frac{1}{12}\left[(U_i^n + U_i^{n-1})\delta_x(U_i^n + U_i^{n-1}) + \delta_x((U_i^n + U_i^{n-1})^2)\right]\\ &\qquad - \delta_t\delta_x^2 U_i^{n-1} + \frac{1}{2}\delta_x(G_i^n + G_i^{n-1}) = 0, \quad i = 1, \cdots, M-1,\\ &\delta_t G_i^n + \frac{1}{2}\delta_x(U_i^n + U_i^{n-1}) = 0, \quad i = 1, \cdots, M-1,\end{aligned}$$

where $\delta_x U_i^n := \frac{U_{i+1}^n - U_{i-1}^n}{2h}$, $\delta_x^2 U_i^n := \frac{U_{i+1}^n - 2U_i^n + U_{i-1}^n}{h^2}$ and h is the uniform spatial grids stepsize.

The exact solitary wave solution of the nonlinear SRLW equation (1)–(2) has the following form [27]

$$u(x,t) = \frac{3\left(v^2-1\right)}{v}\operatorname{sech}^2\left(\sqrt{\frac{v^2-1}{4v^2}}(x - vt)\right), \tag{93}$$

and the exact density is

$$\rho(x,t) = \frac{3\left(v^2-1\right)}{v^2}\,\mathrm{sech}^2\left(\sqrt{\frac{v^2-1}{4v^2}}(x-vt)\right), \tag{94}$$

where v is a wave speed parameter. The existence of bidirectional propagation is allowed, and two branches of solitary waves for the velocity v in the range $v<-1$ and $v>1$ simply refer to left and right traveling solitary waves of the same type.

The non-uniform spatial grids used in this paper are formulated as follows. First, we construct a uniform partition $\{x_{\mathrm{fix},\ i+1/2}\}_{i=0}^{M}$ of the domain with equal grid size $h_{\mathrm{fix}}=(b-a)/M$. Then, by a small random perturbation of the grid size using the Matlab inline code, we define the non-uniform grid points

$$x_{i+1/2} = x_{\mathrm{fix},i+1/2} + \beta * h_{\mathrm{fix}} * [-1+2*rand(i)], \qquad 1\le i\le M-1, \tag{95}$$

where β is a small mesh parameter, which can control the random disturbance within a certain range.

5.1. Accuracy and efficiency test.

Example 5.1. *(A Single Wave). In this example, we take the internal* $x\in[-20,50]$ *and temporal domain* $t\in[0,20]$. *The solitary wave solutions are given by* (93)–(94) *with* $v=\sqrt{2}$, *and the exact flux* p *is computed by taking the derivative of* u *with respect to space, see* (7).

The purpose of this example is to test accuracy of the related methods on uniform and non-uniform spatial grids, respectively, and to show efficiency of the linearized BDF2-BCFD and CN-BCFD methods compared with the fully nonlinear method mentioned above.

TABLE 1. Errors on uniform grid at $t=20$.

Method	h	$\|U_h-u\|_{\mathrm{M}}$	Order	$\|P_h-p\|_{\mathrm{T}}$	Order	$\|G_h-\rho\|_{\mathrm{T}}$	Order	CPU (s)
BDF2-BCFD (11)–(13)	0.2	4.69e-01	-	2.76e-01	-	3.35e-01	-	1
	0.1	1.10e-01	2.09	6.64e-02	2.05	7.92e-02	2.08	5
	0.05	2.53e-02	2.12	1.54e-02	2.11	1.83e-02	2.11	22
	0.025	6.00e-03	2.08	3.60e-03	2.10	4.30e-03	2.10	119
	0.01	9.25e-04	2.04	5.63e-04	2.02	6.71e-04	2.03	1198
CN-BCFD (19)–(21)	0.2	1.85e-01	-	1.11e-01	-	1.32e-01	-	1
	0.1	4.29e-02	2.11	2.59e-02	2.10	3.05e-02	2.11	5
	0.05	1.02e-02	2.07	6.10e-03	2.09	7.30e-03	2.06	20
	0.025	2.50e-03	2.03	1.50e-03	2.02	1.80e-03	2.02	90
	0.01	3.89e-04	2.03	2.35e-04	2.02	2.77e-04	2.04	901

TABLE 2. Errors on uniform grid at $t=20$.

Method	h	$\|U_h-u\|_{\mathrm{T}}$	Order	$\|G_h-\rho\|_{\mathrm{T}}$	Order	CPU Time (s)
Nonlinear method [31]	0.2	1.37e-01	-	1.00e-01	-	3
	0.1	3.47e-02	1.98	2.54e-02	1.98	10
	0.05	8.71e-02	1.99	6.39e-03	1.99	47
	0.025	2.18e-03	2.00	1.60e-03	2.00	287
	0.01	3.49e-04	2.00	2.59e-04	1.98	2579

First, we test the convergence rate and CPU time consumed for the linearized BDF2-BCFD method, the linearized CN-BCFD method as well as the fully nonlinear method on uniform grids. Theoretically, all three schemes are second-order in time and space. Set $\Delta t = h_{\text{fix}}$, and $\beta = 0$ in (95). Tables 1 and 2 show the numerical errors of u, p, ρ and CPU running time. Basically, we have the following observations:

(i) All three methods generate errors of u and ρ measured in the discrete norm (see (10)) in the same order of magnitude, and second-order convergence both in time and space are seen, which are consistent with the conclusions in Theorems 3.2 and 3.3. We can also observe that the methods are stable and the errors are small for $\Delta t = 0.2$, which means that the required condition $\Delta t \leq \frac{1}{1+2L} < 0.2$ (here $L = \frac{3}{\sqrt{2}}$) in Theorem 4.1 is not necessary.

(ii) Compared to the fully nonlinear method [31], our proposed linearized BDF2-BCFD and CN-BCFD methods can calculate u, ρ and p at the same time, and meanwhile the convergence order of p is not reduced.

(iii) The linearized methods are much more efficient (even 2 to 3 times faster) than the nonlinear method. Besides, it seems that the linearized CN-BCFD method is more efficient than the linearized BDF2-BCFD method, as the BDF2 method employed more function values of previous time levels.

FIGURE 1. Non-uniform exemplary grid with $h_{\text{fix}} = 0.2$, $\beta = 0.1$.

Next, we test the convergence rate of the methods on non-uniform grids, where the grids partition are obtained by (95) with $\beta = 0.1$. Figure 1 shows a schematic diagram of non-uniform grids with $h_{\text{fix}} = 0.2$ and $\beta = 0.1$. The short vertical line indicates the uniform division, and the long one represents the corresponding non-uniform partition. As seen there are totally five unequal cells, and it is apparently that the length of the second cell is much larger than that of the others. We shall use the non-uniform grids like Figure 1 to test the two linearized methods. Errors on non-uniform grids are presented in Table 3, in which $\Delta t = h_{\text{fix}}$ and $\beta = 0.1$. Second-order error accuracy in time and space are still observed in this situation, which is also well consistent with the conclusions in Theorems 3.2 and 3.3. But the linearized CN-BCFD method (19)–(21) yields smaller errors than the linearized BDF2-BCFD method (11)–(13). Furthermore, a much smaller grid disturbance with $\beta = 0.05$ is considered. Errors and convergence orders are presented in Table 4. We can see that, as β getting smaller, numerical errors decrease and gradually approach to those in Table 1 on uniform grids.

5.2. Long-time simulations. One of important characteristics of soliton waves is that its waveform does not change with time propagation. Thus, it is essential to observe the behavior of numerical solutions over a long period of time.

Example 5.2. *(Long-time simulations). In this example, we use the same solutions as in Example 5.1, but the spatial internal is chosen as* $x \in [-20, 160]$ *and the temporal domain is taken as* $t \in [0, 100]$.

The waveform obtained by the present two schemes are plotted in Figures 2 and 4, respectively, where $h_{\text{fix}} = 0.1$, $\beta = 0.1$ and $\Delta t = 0.01$. The shape errors of the

TABLE 3. Errors on non-uniform grid at $t = 20$ with $\beta = 0.1$.

Method	h_{fix}	$\|U_h - u\|_{\text{M}}$	Order	$\|P_h - p\|_{\text{T}}$	Order	$\|G_h - \rho\|_{\text{T}}$	Order
BDF2-BCFD (11)–(13)	0.2	4.74e-01	-	2.77e-01	-	3.36e-01	-
	0.1	1.11e-01	2.08	6.67e-02	2.05	7.97e-02	2.08
	0.05	2.55e-02	2.12	1.55e-02	2.11	1.85e-02	2.11
	0.025	6.00e-03	2.09	3.70e-03	2.07	4.50e-03	2.04
	0.01	9.31e-04	2.04	6.03e-04	1.98	7.57e-04	1.95
CN-BCFD (19)–(21)	0.2	1.87e-01	-	1.13e-01	-	1.33e-01	-
	0.1	4.35e-02	2.10	2.64e-02	2.10	3.13e-02	2.09
	0.05	1.04e-02	2.06	6.40e-03	2.04	7.70e-03	2.02
	0.025	2.50e-03	2.06	1.60e-03	2.00	2.00e-03	1.94
	0.01	3.96e-04	2.01	2.63e-04	1.97	3.33e-04	1.96

TABLE 4. Errors on non-uniform grid at $t = 20$ with $\beta = 0.05$.

Method	h_{fix}	$\|U_h - u\|_{\text{M}}$	Order	$\|P_h - p\|_{\text{T}}$	Order	$\|G_h - \rho\|_{\text{T}}$	Order
BDF2-BCFD (11)–(13)	0.2	4.69e-01	-	2.76e-01	-	3.35e-01	-
	0.1	1.10e-01	2.09	6.65e-02	2.05	7.92e-02	2.08
	0.05	2.54e-02	2.12	1.54e-02	2.11	1.83e-02	2.11
	0.025	6.00e-03	2.08	3.65e-03	2.07	4.36e-03	2.07
	0.01	9.25e-04	2.04	5.66e-04	2.03	6.83e-04	2.02
CN-BCFD (19)–(21)	0.2	1.85e-01	-	1.12e-01	-	1.32e-01	-
	0.1	4.29e-02	2.11	2.59e-02	2.10	3.06e-02	2.11
	0.05	1.02e-02	2.07	6.16e-03	2.07	7.30e-03	2.07
	0.025	2.50e-03	2.03	1.50e-03	2.04	1.80e-03	2.02
	0.01	3.90e-04	2.02	2.42e-04	1.99	3.05e-04	1.94

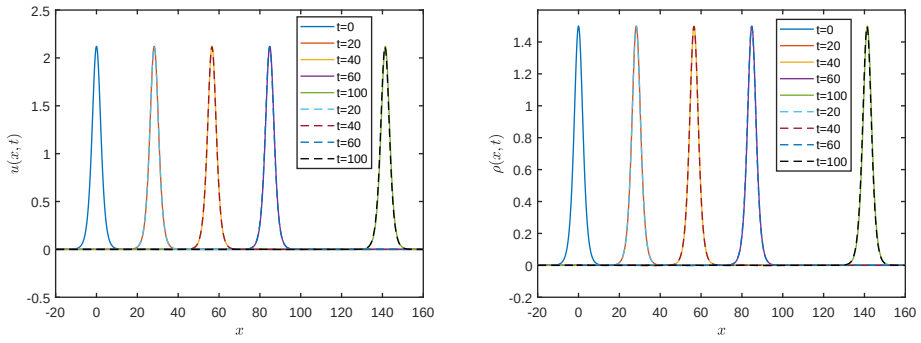

FIGURE 2. Numerical (dash line) and exact (full line) solutions of $u(x,t)$ (left) and $\rho(x,t)$ (right) with $\Delta t = 0.01$, $h_{\text{fix}} = 0.1$ for BDF2-BCFD.

numerical solutions at different times are also depicted in Figures 3 and 5. It can be observed that

(i) The waveforms at different time instants $t = 20$, 40, 60 and 100 all agree with the waveforms at $t = 0$ quite well.

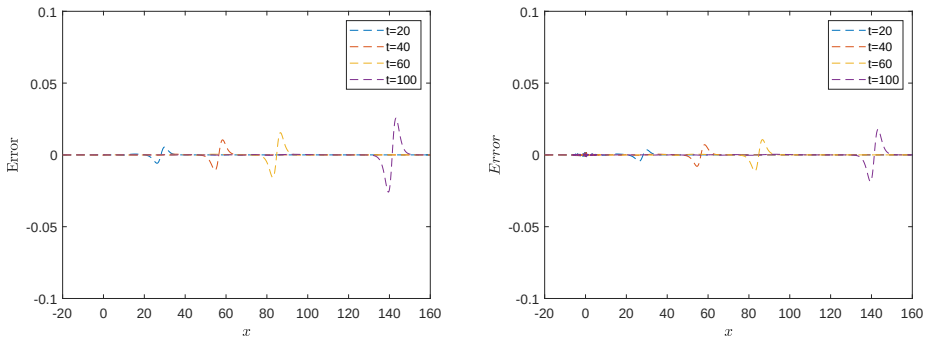

FIGURE 3. Error plots of $u(x,t)$ (left) and $\rho(x,t)$ (right) at different time with $\Delta t = 0.01$, $h_{\text{fix}} = 0.1$ for BDF2-BCFD.

(ii) Although the errors of $u(x,t)$ and $\rho(x,t)$ increase with respect to time, they remain the magnitude of 10^{-2} when $t = 100$.

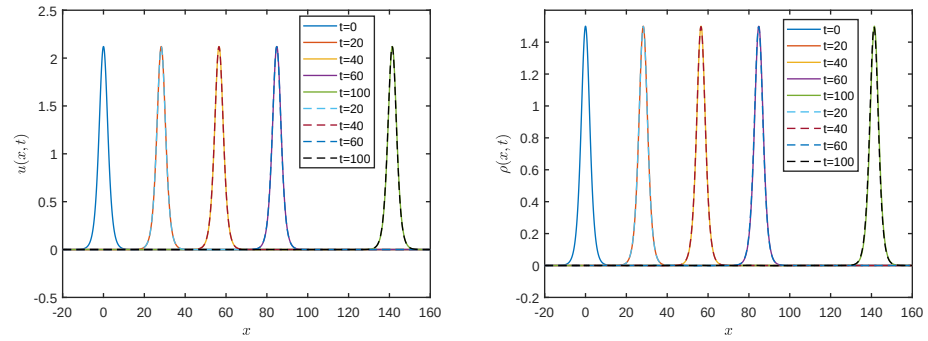

FIGURE 4. Numerical (dash line) and exact (full line) solutions of $u(x,t)$ (left) and $\rho(x,t)$ (right) with $\Delta t = 0.01$, $h_{\text{fix}} = 0.1$ for CN-BCFD.

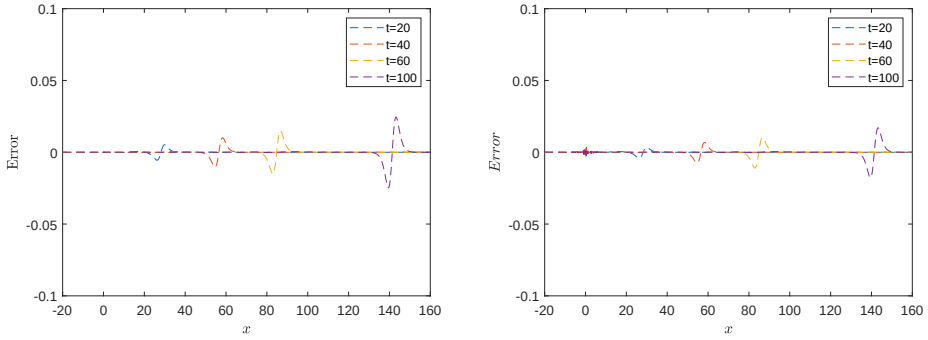

FIGURE 5. Error plots of $u(x,t)$ (left) and $\rho(x,t)$ (right) at different time with $\Delta t = 0.01$, $h_{\text{fix}} = 0.1$ for CN-BCFD.

In conclusion, the numerical solutions obtained by our developed schemes always have the characteristic of the exact soliton wave solutions. Therefore, both the accuracy and stability of the linearized BDF2-BCFD and CN-BCFD schemes are guaranteed.

5.3. Collision of two solitons. Finally, we examine the performance of the present schemes for the collision of solitons. Results from a sequence of numerical simulations in cases of co-propagating interaction between two solitons are presented as follows.

Example 5.3. *(Collision of two solitons). In this example, we take the spatial interval* $x \in [-60, 120]$ *and the temporal domain* $t \in [0, 20]$. *The initial conditions associated with the collision of two solitons are given by*

$$\begin{aligned} u_0(x) =& \frac{3\left(v_1^2-1\right)}{v_1}\operatorname{sech}^2\left(\sqrt{\frac{v_1^2-1}{4v_1^2}}\,(x-x_0)\right) \\ &+ \frac{3\left(v_2^2-1\right)}{v_2}\operatorname{sech}^2\left(\sqrt{\frac{v_2^2-1}{4v_2^2}}\,(x+x_0)\right), \\ \rho_0(x) =& \frac{3\left(v_1^2-1\right)}{v_1^2}\operatorname{sech}^2\left(\sqrt{\frac{v_1^2-1}{4v_1^2}}(x-x_0)\right) \\ &+ \frac{3\left(v_2^2-1\right)}{v_2^2}\operatorname{sech}^2\left(\sqrt{\frac{v_2^2-1}{4v_2^2}}(x+x_0)\right). \end{aligned}$$

In the simulation, we set the parameters $v_1 = 2$, $v_2 = 6$ and $x_0 = 12$. First, we test the convergence rate of the two methods on non-uniform grids generated by (95) with $\beta = 0.1$. Since no exact solutions are available for this example, the errors are measured by the so-called Cauchy error [8], which is calculated between solutions obtained on two adjacent grid pairs $(\Delta t, h_{\text{fix}})$ and $(\Delta t/2, h_{\text{fix}}/2)$ by $\|e_U\|_{\text{M}} = \|U^{\Delta t}_{h_{\text{fix}}} - U^{\Delta t/2}_{h_{\text{fix}}/2}\|_{\text{M}}$, where $U^{\Delta t}_{h_{\text{fix}}}$ denotes the numerical solution under temporal stepsize Δt and spatial stepsize h_{fix} ($\|e_P\|_{\text{T}}$ and $\|e_G\|_{\text{T}}$ are similarly defined). The numerical results of the discrete L^2 Cauchy errors on the non-uniform spatial grids are presented in Table 5, and from which we can also confirm the second-order temporal and spatial convergences for both the variables u, p and ρ.

TABLE 5. Errors on non-uniform grid at $t = 1$ with $\beta = 0.1$.

Method	$\Delta t = h_{\text{fix}}$	$\|e_U\|_{\text{M}}$	Order	$\|e_P\|_{\text{T}}$	Order	$\|e_G\|_{\text{T}}$	Order
BDF2-BCFD (11)–(13)	0.02	3.00e-01	-	2.47e-01	-	5.00e-02	-
	0.01	6.68e-02	2.17	5.64e-02	2.13	1.20e-02	2.06
	0.025	1.54e-02	2.12	1.32e-02	2.10	3.00e-03	2.00
CN-BCFD (19)–(21)	0.02	1.12e-01	-	9.09e-02	-	2.00e-02	-
	0.01	2.56e-02	2.12	2.10e-02	2.11	5.00e-03	2.00
	0.005	6.10e-03	2.07	5.10e-03	2.04	1.20e-03	2.06

Next, we model the collision of the two solitons. The spatial and temporal meshes are constructed via choosing $h_{\text{fix}} = 0.05$, $\beta = 0.1$ in (95) and $\Delta t = 0.001$. It is clear that the initial two waves are centered at $x = -12$ and 12, with speed $v_2 = 6$ and $v_1 = 2$, respectively. As time marching from $t = 0$ to $t = 20$, the

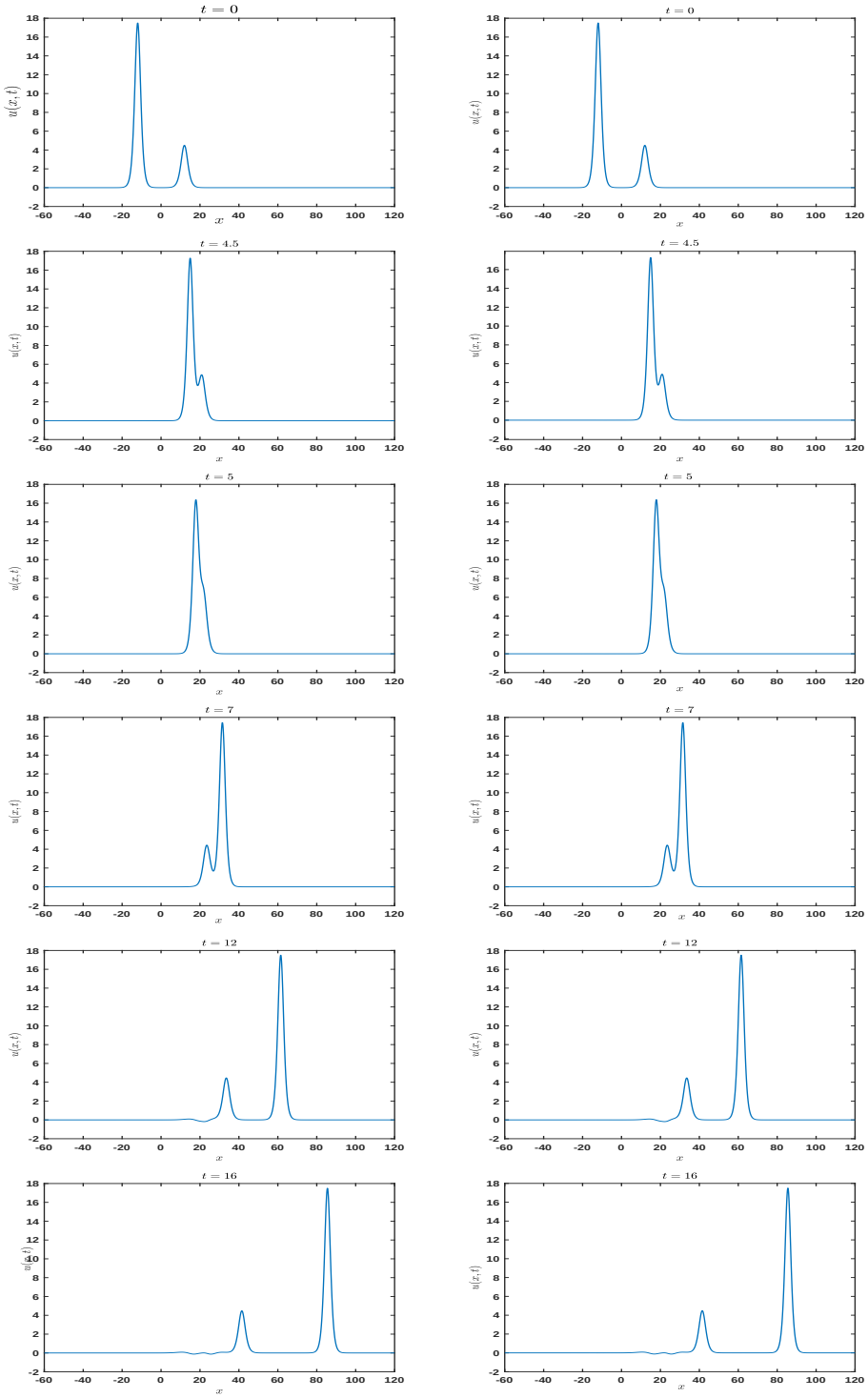

FIGURE 6. Collision of two waves for BDF2-BCFD (left) and CN-BCFD (right) with $\Delta t = 0.001$, $h_{\text{fix}} = 0.05$.

two waves gradually merge into a whole one, and then the faster wave moves and overtakes the slower one. Finally, the two waves return back to the original shape, respectively, see Figure 6.

6. Conclusions

In this paper, two linearized BCFD algorithms named BDF2-BCFD (see, (11)–(13)) and CN-BCFD (see, (19)–(21)) for the modeling of nonlinear SRLW equation are presented. Under a reasonable restriction on the time stepsize, we prove that both algorithms have second-order temporal and spatial accuracy on either uniform or non-uniform spatial grids. Finally, the methods are utilized to simulate the physical motions of a single wave and two solitary waves, also used for long-time simulations. Moreover, Collision of two soliton waves with different wave speed on non-uniform spatial grids are also tested, which show that the proposed methods can maintain the waveform and wave speed very well. Recently, He et al. [15] proposed a new linearized fourth-order conservative compact difference scheme for the SRLW equations under periodic boundary conditions, which inspired us to study two-grid fourth-order compact difference methods for the nonlinear SRLW equation in the future.

Acknowledgements

This work was supported in part by the National Natural Science Foundation of China (Nos. 11971482, 12131014), by the Fundamental Research Funds for the Central Universities (Nos. 202264006, 202261099) and by the OUC Scientific Research Program for Young Talented Professionals.

References

[1] T. Arbogast, M.F. Wheeler, I. Yotov, Mixed finite elements for elliptic problems with tensor coefficients as cell-centered finite differences, SIAM J. Numer. Anal. 34 (1997), 828–852.
[2] V. Benci, Quantum Phenomena in a Classical Model, Found. Phys. 29 (1999), 1–28.
[3] C. Bridges, K.R. Rajagopal, Pulsatile Flow of a Chemically-Reacting Nonlinear Fluid, Comput. Math. Appl. 52 (2006), 1131–1144.
[4] Y. Bai, L. Zhang, A conservative finite difference scheme for generalized symmetric regularized long wave equations, Acta Math. Appl. Sin. 35 (2012), 458–470.
[5] L. Chen, Stability and instability of solitary wave for generalized symmetric regularized long wave equations, Phys. D Nonlinear Phenom. 118 (1998), 53–68.
[6] P. A. Clarkson, New similarity reductions and Painleve analysis for the symmetric regularised long wave and modified Benjamin-Bona-Mahoney equations, J. Phys. Math. General 22 (1989), 3821–3848.
[7] N. Cheemaa, A.R. Seadawy, S. Chen, Some new families of solitary wave solutions of the generalized Schamel equation and their applications in plasma physics, Eur. Phys. J. Plus 134 (2019), 117.
[8] A. Diegel, X. Feng, S. Wise, Analysis of a mixed finite element method for a Cahn-Hilliard-Darcy-Stokes system. SIAM J. Numer. Anal. 53 (2015) 127–152.
[9] S. Fang, B. Guo, Q. Hua, The existence of global attractors for a system of multi-dimensional symmetric regularized wave equations, Commun. Nonlinear Sci. Numer. Simul. 14 (2009), 61–68.

[10] B. Guo, The spectral method for symmetric regularized wave equations, J. Comput. Math. 4 (1987), 297–306.
[11] Y. Gao, L. Mei, Galerkin finite element methods for two-dimensional RLW and SRLW equations, Appl. Anal. 97 (2018), 2288–2312.
[12] J. Hu, K. Zheng, M. Zheng, Numerical simulation and convergence analysis of a high-order conservative difference scheme for SRLW equation, Appl. Math. Model. 38 (2014), 5573–5581.
[13] Y. He, X. Wang, H. Chen, Y. Deng, Numerical analysis of a high-order accurate compact finite difference scheme for the SRLW equation, Appl. Math. Comput. 418 (2022), 126837.
[14] Y. He, X. Wang, W. Dai, Coupled and decoupled high-order accurate dissipative finite difference schemes for the dissipative generalized symmetric regularized long wave equations, Numer. Methods Partial Differ. Equ. 38 (2021), 1112–1143.
[15] Y. He, X. Wang, R. Zhong, A new linearized fourth-order conservative compact difference scheme for the SRLW equations, Adv. Comput. Math. 48 (2022), 27.
[16] B. Ji, L. Zhang, Q. Sun, A dissipative finite difference Fourier pseudo-spectral method for the symmetric regularized long wave equation with damping mechanism, Appl. Numer. Math. 154 (2020), 90–103.
[17] Y. Jin, F. Liao, J. Cai, Compact schemes for multiscale flows with cell-centered finite difference method, J. Sci. Comput. 85 (2020), 17.
[18] L. Kong, W. Zeng, R. Liu, L. Kong, Multisymplectic Fourier pseudo-spectral scheme for the SRLW equation and conservation laws, Chinese J. Comput. Phys. 23 (2006), 25–31.
[19] S. Li, Numerical study of a conservative weighted compact difference scheme for the symmetric regularized long wave equations, Numer. Methods Partial Differ. Equ. 35 (2018), 60–83.
[20] Y. Liu, Y. Shi, D.A. Yuen, et al., Comparison of linear and nonlinear shallow wave water equations applied to tsunami waves over the China Sea, Acta Geotech. 4 (2009), 129–137 .
[21] S. Li, X. Wu, L_∞ error bound of conservative compact difference scheme for the generalized symmetric regularized long-wave (GSRLW) equations, Comput. Appl. Math. 37 (2018), 2816–2836.
[22] R. C. Mittal, A. Tripathi, Numerical solutions of symmetric regularized long wave equations using collocation of cubic B-splines finite element, Int. J. Comput. Methods Eng. Sci. Mech. 16 (2015), 142–150.
[23] Z. Meng, L. Yang, L. Hong, Fully discrete two-step mixed element method for the symmetric regularized long wave equation, Int. J. Model. Simul. Sci. Comput. 5 (2014), 1450007.
[24] T. Nie, A decoupled and conservative difference scheme with fourth-order accuracy for the symmetric regularized long wave equations, Appl. Math. Comput. 219 (2013), 9461–9468.
[25] H. Rui, H. Pan, A block-centered finite difference method for the Darcy-Forchheimer model, SIAM J. Numer. Anal. 50 (2012), 2612–2631.
[26] P.A. Raviart, J.M. Thomas, A mixed finite element method for 2nd order elliptic problems. In: Mathe-matical Aspects of Finite Element Methods, Springer Berlin Heidelberg, (1977), 292–315.
[27] C.E. Seyler, D.L. Fenstermacher, A symmetric regularized-long-wave equation, Phys. Fluids 27 (1984), 4–7.

[28] Y. Shang, B. Guo, Analysis of Chebyshev pseudospectral method for multi-dimensional generalized SRLW equation, Appl. Math. Mech. 24 (2003), 1168–1183.
[29] M. V. Tratnik, Twisted solitons in birefringent optical fibers, Opt. Lett. 17 (1992), 917–919.
[30] A. Weiser, M.F. Wheeler, On convergence of block-centered finite differences for elliptic problems, SIAM J. Numer. Anal. 25 (1988), 351–375.
[31] T. Wang, L. Zhang, F. Chen, Conservative schemes for the symmetric regularized long wave equations, Appl. Math. Comput. 190 (2007), 1063–1080.
[32] F. Xu, Application of Exp-function method to symmetric regularized long wave (SRLW) equation, Phys. Lett. A 372 (2008), 252–257 .
[33] J. Xu, S. Xie, H. Fu, A two-grid block-centered finite difference method for the nonlinear regularized long wave equation, Appl. Numer. Math. 171 (2022), 128–148.
[34] Y. Xu, B. Hu, X. Xie, J. Hu, Mixed finite element analysis for dissipative SRLW equations with damping term, Appl. Math. Comput. 218 (2012), 4788–4797.
[35] Y. Yuan, Y. Liu, C. Li, T. Sun, L. Ma, Analysis on block-centered finite differences of numerical simulation of semiconductor device detector, Appl. Math. Comput. 279 (2016), 1–15.
[36] S. Yimnet, B. Wongsaijai, T. Rojsiraphisal, K. Poochinapan, Numerical implementation for solving the symmetric regularized long wave equation, Appl. Math. Comput. 273 (2016), 809–825.
[37] X. Zhao, An exponential wave integrator pseudospectral method for the symmetric regularized-long-wave equation, J. Comput. Math. 1 (2016), 49–69.
[38] J. Zheng, R. Zhang, B. Guo, The Fourier pseudo-spectral method for the SRLW equation, Appl. Math. Mech. 10 (1989), 801–810.

School of Mathematical Sciences, Ocean University of China, Qingdao, Shandong 266100, China

E-mail: jxu129@163.com

School of Mathematical Sciences, Ocean University of China, Qingdao, Shandong 266100, China & Laboratory of Marine Mathematics, Ocean University of China, Qingdao, Shandong 266100, China

E-mail: shusenxie@ouc.edu.cn and fhf@ouc.edu.cn